ADVANCED CONCEPTS AND TIME TRANSFER SESSION SUMMARY

Chair: Hiroo Kunimori

New applications using all or part of SLR instrumentation were the subjects of papers presented in this session. SLR was born and has grown up in the fields of geodesy, geodynamics, and orbital mechanics, and since then has interacted with many other fields to open up new applications and users. In addition to the obvious value of SLR as a contributor to fundamental physics, geodesy and the reference frame, each organization has its own interests to use SLR for different applications. Here we have 5 oral papers and 3 poster papers including Time Transfer, Communications, Radio Astronomy, Lidar and NEO Tracking.

Time Transfer

"Progress on Laser Time Transfer Project" by Y. Fumin et al described the China LTT mission on a satellite, hopefully to be approved in the next three months. It uses dual SPAD, TDC module and Laser Retroreflector Array. The engineering model and testing are in progress. The experiment is now planned only within the China network.

"T2L2 Status Update" by E. Samain, F. Deleflie et al gave news of the Time Transfer by Laser Link project, a LASSO follow-on mission at last approved for the JASON-2 mission for 2008 launch, 30 years after the concept was made. Tests using the space segment engineering model and the ground prototype are ongoing, and an international network is being modelled.

"New Application of KHz Laser Ranging: Time Transfer by Ajisai" by T. Otsubo et al presented a simulation study for AJISAI TT revised 14 years after the concept was introduced in equation form, including a search algorithm and link budget in the KHz SLR era.

Communications

"Satellite Tracking Demonstration on Ground Using 100mm Aperture Optical Antenna for Space Laser Communication" by H. Kunimori et al described how SLR using optical communications equipment were present in a course of development of a next-generation Laser Comm terminal, and present-generation LEO-GND Laser Comm was described.

Also, in another session, a free space Laser Comm experiment over ocean over 10 miles was presented.

Radio Astronomy

"Possibility of Laser Ranging Support for the Next-Generation Space VLBI Mission ASTRO-G" by T. Otsubo et al discussed the role of SLR in POD at altitudes higher than GPS, and the engineering problems.

LIDAR

"LIDAR Experiments at the Space Geodesy Facility, Herstmonceux, UK" by G. Appleby et al.

NEO Tracking and Monitoring

"Electron Multiplying CCD Camera Performance Tests" by D. Lewova et al.

"Possibility of Near Earth Objects Distance Measurement with Laser Ranging Device" by M. Abele and L. Osipova.

Progress on Laser Time Transfer Project

Yang Fumin[1], Huang Peicheng[1], Chen Wanzhen[1], Zhang Zhongping[1],
Wang Yuanming[1], Chen Juping[1], Guo Fang[1],Zou Guangnan[2], Liao Ying[2],
Ivan Prochazka[3], Karel Hamal[3]

1. Shanghai Observatory, Chinese Academy of Science, Shanghai, China
2. China Academy of Space Technology, Beijing, China
3. Czech Technical University in Prague, Czech Republic

Abstract

The purposes of the Laser Time Transfer (LTT) experiment are to synchronize the atomic clocks in space to ones on the ground, and to verify the relativity theory. The LTT payload in space includes a dual-SPAD detector, a timer based on TDC device, control unit and a LRA. The expected uncertainty of measurement of clock differences for single shot is about 200ps, and the uncertainty of measurement for the relative frequency differences for two rubidium clocks is about 5×10^{-14}/ 1000 seconds. The LTT flight module is ready and is waiting for the flight mission in 2007-2008.

Introduction

Based on the successful time transfer by laser pulses between ground stations in 2003[1], the Laser Time Transfer (LTT) project between satellite and ground stations was initiated in 2004. The goals of the LTT are as follows: 1) Evaluation of performance of space clocks which are rubidium's now, and will be hydrogen clocks in the future. 2) Verification of the relativity

Shanghai Astronomical Observatory, in cooperation with the China Academy of Space Technology in Beijing, has been in charge of the LTT project. The Philosophy of the project is to make a payload as simple as possible on a satellite in a short time to verify the capability of the time transfer by laser pulses between space and ground clocks. So, a simple 40um SPAD detector with 100ps timing resolution[2] and the TDC devices with lower resolution(125ps)[3] have been chosen for the space module. The LTT project has kept going smoothly since 2004. The flight module has been built and has passed the space environmental testings.

Principle of LTT

Fig.1. shows the principle of LTT. ΔT –time difference of second pulses between space and ground clocks. T_G – time interval between the transmitting laser pulse and second pulse of the ground clock. T_S – time interval between the received laser pulse and second pulse of the space clock. τ – flight time of laser pulse between ground station and satellite. So we have:

$$\Delta T = \frac{\tau}{2} - T_G - T_S$$

where the relativity effect, system delays, atmospheric correction and so on are not included.

Fig.2. shows the block diagram of LTT. There are three main parts onboard: detector, timer and retro-reflectors.

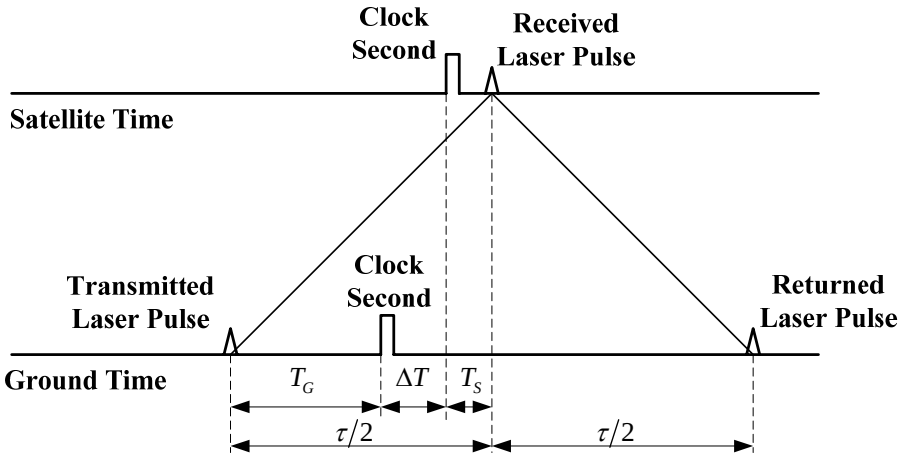

Fig.1. *Principle of Laser Time Transfer*

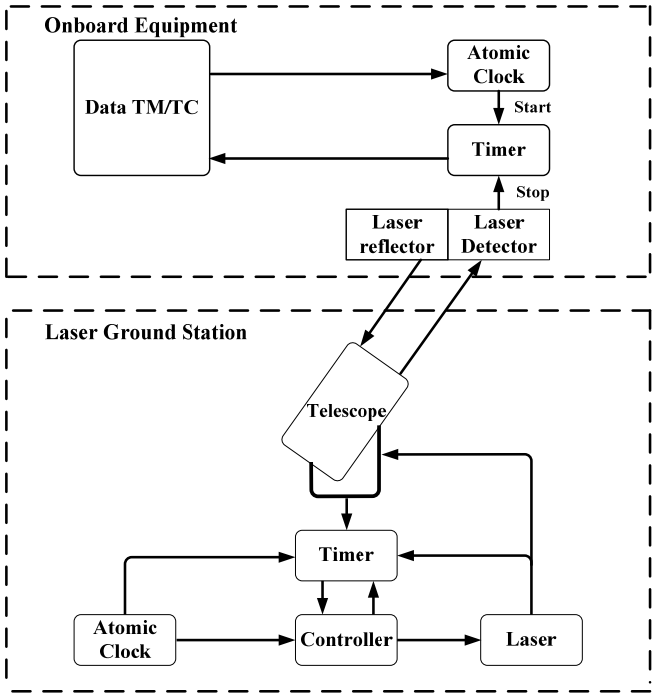

Fig.2. *Diagram of LTT*

Specifications of space module

Laser Reflector Array (LRA)

The LTT module will be installed on the satellite with an orbital altitude of about 20000km. The LRA made by Shanghai Astronomical Observatory has a planar panel with 42 retros. The single retro has an aperture of 33mm without coating on back surfaces. The LRA has the reflective area of 360cm2, and total mass of 2.5kg.

LTT module

Fig.3. is the block diagram of the LTT module. The detector is 40um SPAD made by the Czech Technical University.

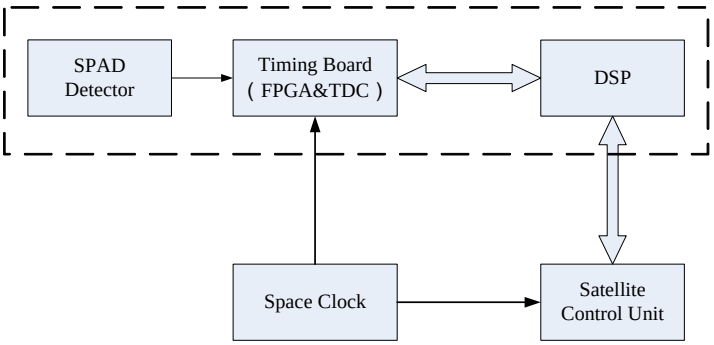

Fig.3. *Block Diagram of LTT Module*

The Specification of the detector is as follows:

- Configuration dual photon counting detector based on Silicon K14 SPAD
- active area circular 25 um diameter
- timing resolution < 100 psec
- operating temp. -30ºC~ +60ºC, no cooling, no stabilisation
- power consumption < 400 mW
- optical damage th. full Solar flux 100 nm BW > 8 hr
- lifetime in space > 5 years

Fig.4. shows the LTT detector. There are two SPAD detectors in the box, one is for spare part and can be switched by telecontrol command from ground. There aren't any lenses in front of the SPAD chips, so the receiving area on board is 40um SPAD chip only. The field of view of the detector is about 30º. There is a 10nm bandwidth filter in front of the SPAD chips.

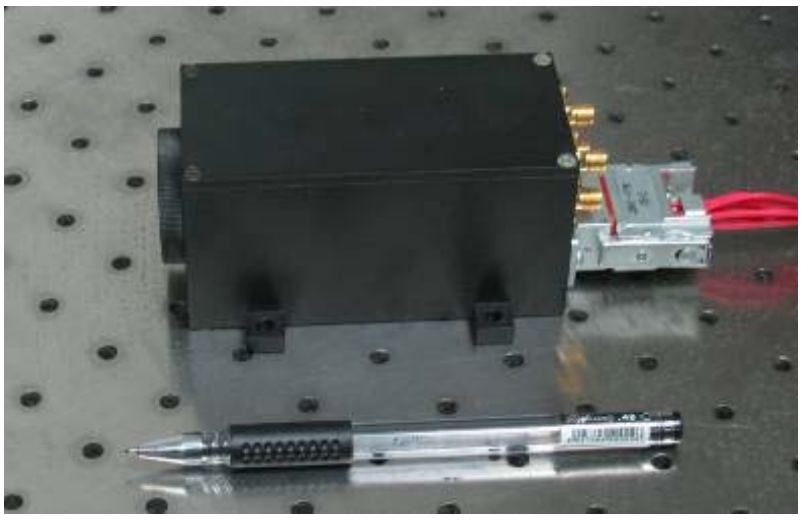

Fig.4. LTT Detector

The received photons onboard NP can be estimated by:

$$N_P = \frac{4 \cdot E \cdot S \cdot A_P \cdot K_t \cdot K_r \cdot T \cdot \alpha}{\pi \cdot R^2 \cdot \theta_t^2}$$

where

E: Laser pulse energy, 50mJ (532nm)

S: Number of photons per joule (532nm), 2.7×10^{18}

A_P: 40μm SPAD without any lenses, diameter of active area, 0.025mm
Kt: Eff. of transmitting optics, 0.60
Kr: Eff. of receiving optics, 0.60
T: Atmospheric transmission (one way), 0.55
R: Range of satellite, for MEO orbit at elevation 30°, 22600Km
θt: Divergency of laser beam from telescope, 10 arcsec
α: Attenuation factor, 0.5

We have, Np=7.0 (Photons)

It can be detected by the 40 μm SPAD detector.

The principle of the LTT timer is shown in Fig.5. The main device is TDC (Time Digit Converter) made by ACAM company in Germany. The TDC-GP1 with resolution of 125ps which had passed the radiation testing in Germany was adopted. Fig.6. shows the LTT timer.

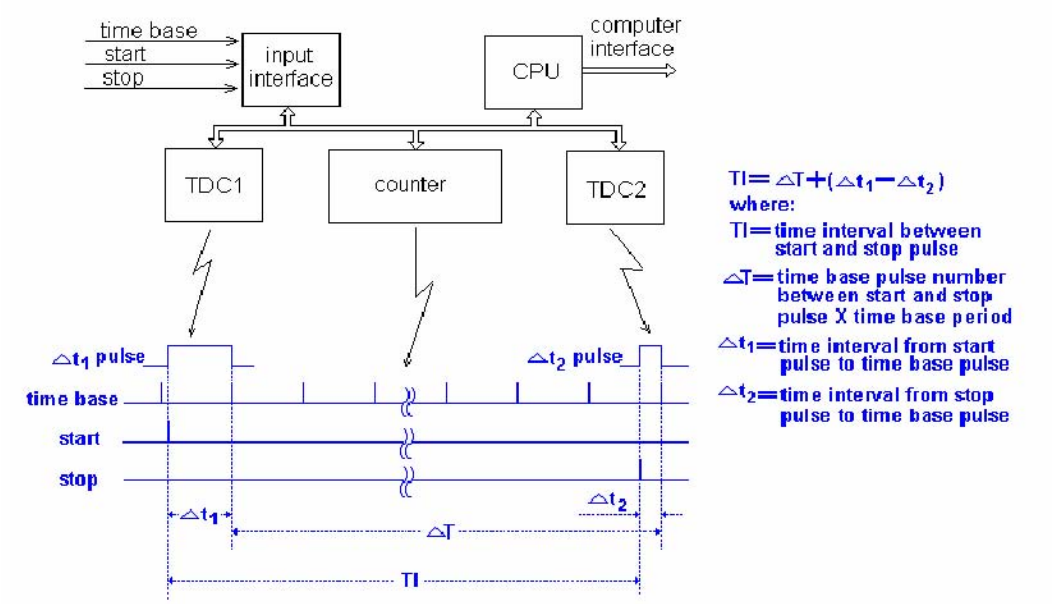

Fig.5. *Principle of the LTT Timer*

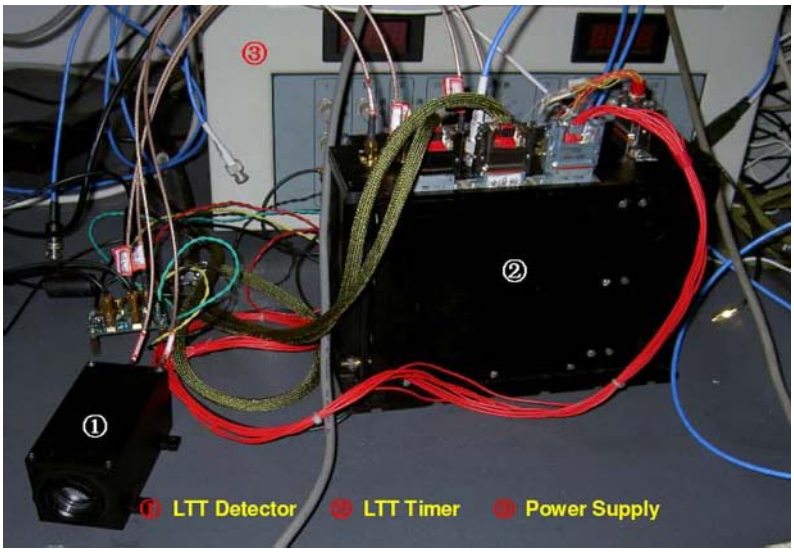

Fig.6. *LTT Timer and Detector*

The specification of the LTT timer is as follows:

- Resolution of timing 10ps
- Precision of timing 100ps
- Mass (dual-timer) 4.3Kg
- Power consumption 17W
- Size 240×100×167mm

Laser firing control for ground stations

For simplification of the module, a 40um SPAD detector without gating circuit and cooling was adopted. In order to keep from the noises produced by the albedo of the ground and the atmosphere, and the detector itself, the ground station will be asked to control strictly the laser firing epoch according to the flight time from ground station to the detector onboard, and let the laser signals arrive at the detector just after the second pulses of the clock onboard, which will start the timer onboard, by 200 ns or so. The laser pulses will stop the timer. So, it is equal to have a gate onboard.

To meet the timing requirement, the laser on the ground station should be actively switched, and the passive switch (or active-passive) can not be used. The accuracy of the prediction of the satellite's range will be about 10m, it equals to 67ns. The uncertainty of laser firing pulses can be controlled within 10ns. The prediction of the difference between the space clock's second and the ground clock's one will be better than 20ns. So we can actually control the received laser pulses with relative to the second pulses of the space clock. Therefore, it means that the time intervals among the laser firings at the station are not constant, and will vary with the distances between the ground station and the satellite.

Ground testing for timing accuracy of LTT module

Fig.7. is the block diagram for the ground testing on the timing accuracy of the LTT module. The specifications of the equipment for the testing are as follows:

- MicroChip Laser
  - Output performance
    - Output power 3μJ
    - Pulse width 650ps
  - Repetition rate 1-100Hz
  - Dimensions (L×W×H) 150×36.4×31mm
  - Weight: 250g
- Rubidium Standard 2 sets, Datum 8000
- Counter (SR620) 2 sets, Stanford Research

Fig.8. and Fig.9. show the instruments for the testing. Table 1 shows the measurement results of the ground testing.

As shown in Table 1, the accuracy of the time difference measurement is 196ps (rms). In Fig.10, line 1 is the result of clock differences by LTT, and line 2 is by the timer SR620 directly. The slope rates of the two lines are: -2.3279×10^{-10} and -2.3285×10^{-10} respectively, and they are coincident very well.

Fig.11. shows several LTT results with 2 sets of Rb clock. The uncertainty for measuring relative frequency difference is about 4×10^{-13} in 200 second and about 5×10^{-14} in 1000 seconds.

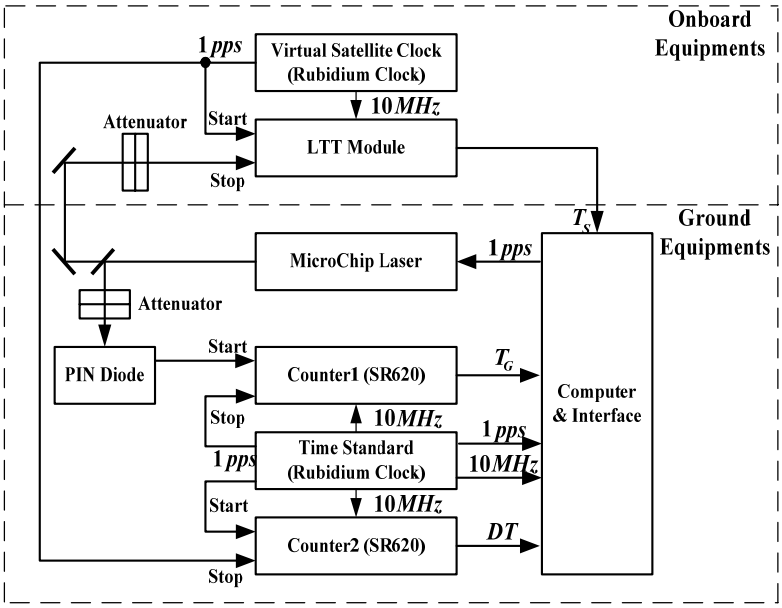

Fig.7. *Diagram of the Testing*

Fig.8. *Ground Testing Instruments*

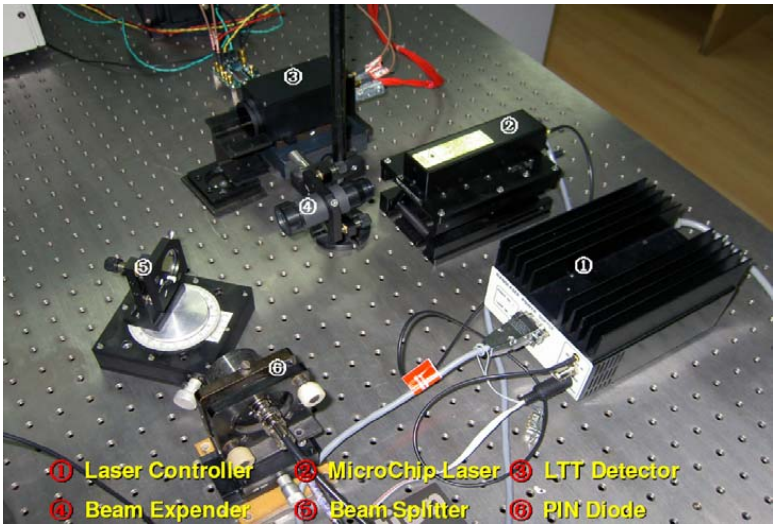

Fig.9. *MicroChip Laser and transmitting Optics*

Table1. *Result of the Ground Testing*

Epoch(s)	(1) Clock Difference by Laser(ns)	(2) Clock Difference by Counter (ns)	(1) (2) (ns)	RMS(ps)	Number of Measurement
3508.7	250300.4	250264.7	35.754	178.4	104
3953.8	250196.3	250160.5	35.783	190.6	139
4246.1	250128.3	250092.6	35.742	165.3	136
4588.9	250048.6	250012.8	35.748	266.7	148
5022.8	249946.8	249911.1	35.751	212.9	84
5498.9	249836.3	249800.5	35.792	73.1	56
5736.5	249781.4	249745.7	35.731	231.2	96
5923.8	249737.7	249702.0	35.687	224.1	103
6187.9	249676.3	249640.7	35.619	199.8	90
6374.8	249633.0	249597.5	35.488	221.6	96
Mean			35.709±0.092	196.4	

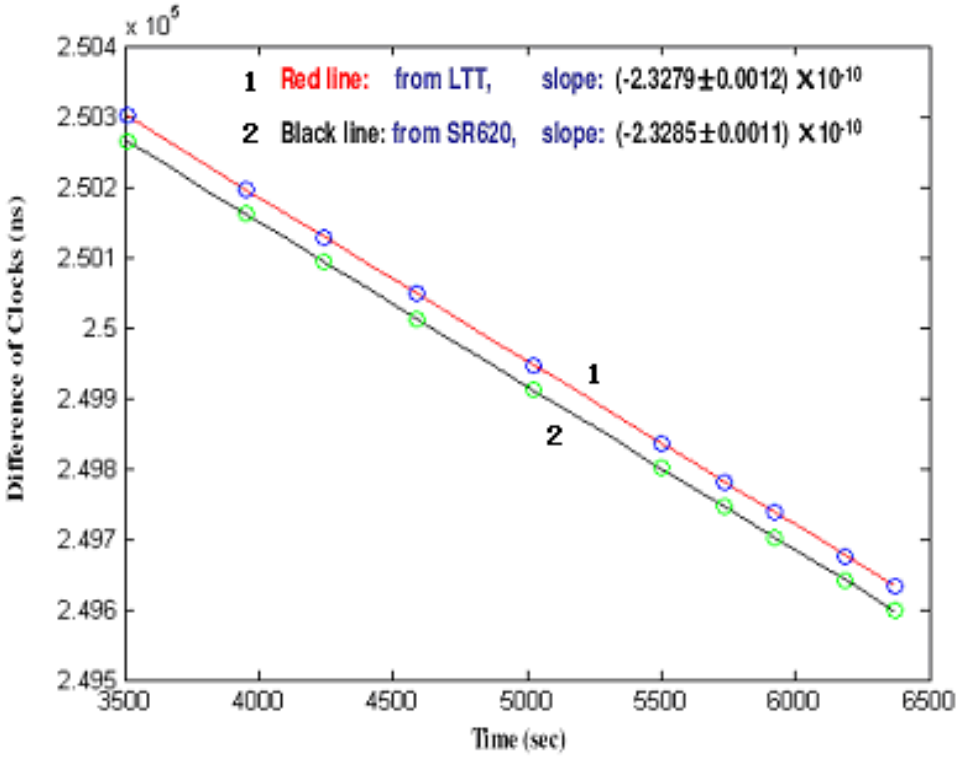

Fig.10. *Results of LTT with two Rb Clocks*

Space Environment Testing

The LTT module has passed the following testing: vibrations, shock, acceleration, thermal circulation, -40--65ºC, thermal vacuum, -40--65ºC, EMC and long term testing in high temperature.

Conclusions

The flight module for Laser Time Transfer experiment has been completed and is waiting for the mission 2007-2008. With the built-in spare parts together, the characteristics of the flight module are as follows:

- Mass 4.6Kg
- Power consumption 17W
- Dimensions:

- 240×100×167mm (dual-timer, interfaces and power supply)
- 105×70×50mm (dual-detector)

- Uncertainty of measurement for the relative frequency differences by laser link for two rubidium standards:
  - 4.0×10^{-13} in 200 seconds
  - 5×10^{-14} in 1000 seconds

References

[1] Yang Fumin, Zhang Zhongping, Chen Wanzhen, Li Xin, Chen Juping, Wang Bin, Time Transfer by Laser Pulses between Ground Stations, 14th International Workshop on Laser Ranging, San Fernando, Spain, 7-11 June, 2004

[2] Ivan Prochazka, Karel Hamal, Lukas Kral, Yang Fumin, Photon Counting Module for Laser Time Transfer Space Mission, 15th International Workshop on Laser Ranging, Canberra, Australia, 15-20 October, 2006

[3] TDC-GP1 User Guide, http://www.acam.de/Documents/English/DB_GP1_e.pd

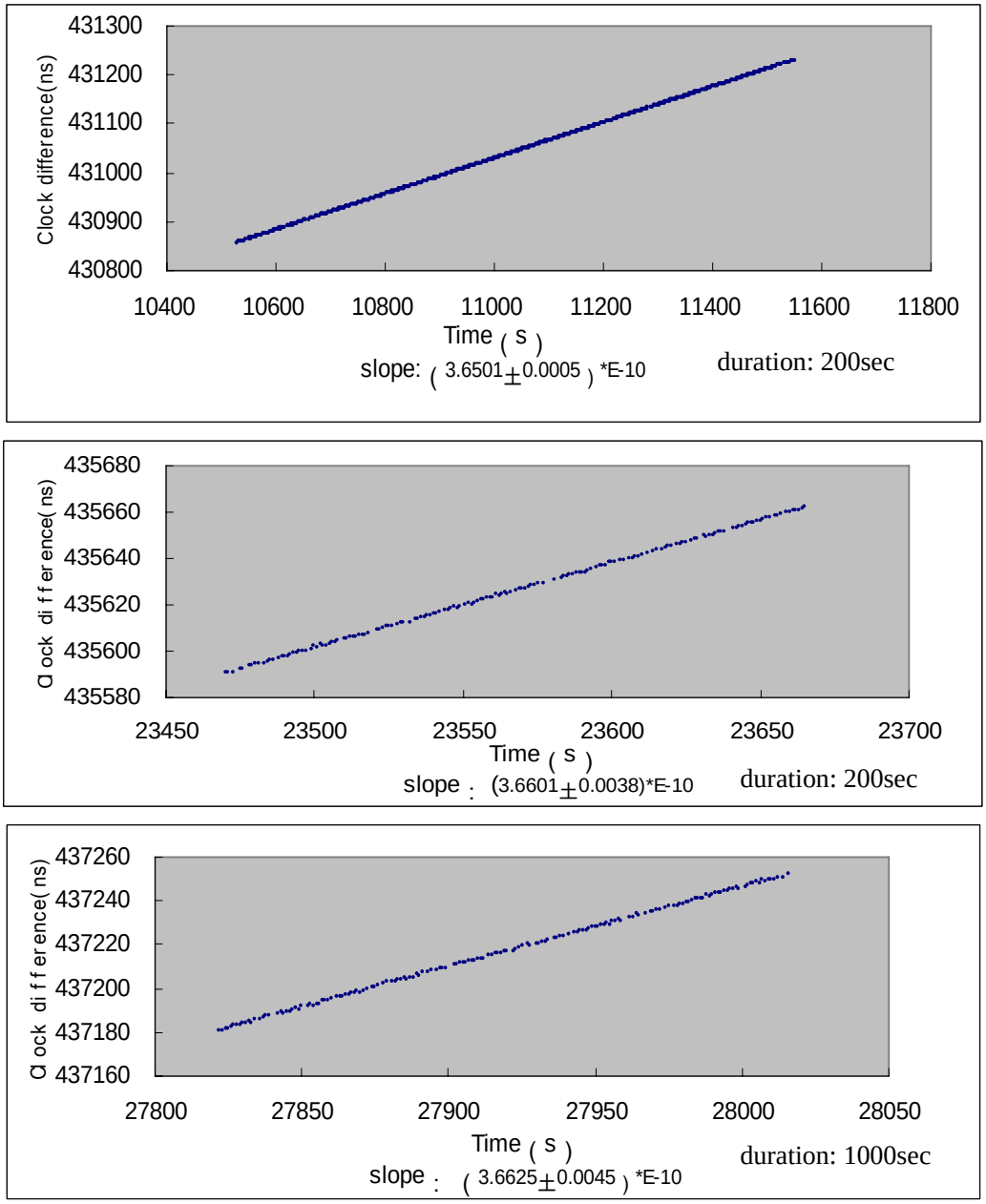

Fig.11. *LTT Results with 2 sets of Rb Clock*

T2L2 – Time Transfer by Laser Link

E. Samain[1], Ph. Guillemot[2], D. Albanese[1], Ph. Berio[1], F. Deleflie[1], P. Exertier[1], F. Para[1], F. Pierron[1], J. Paris[1], I. Petitbon[2], J.-M. Torre[1], P. Vrancken[1], J. Weick[1]

1. OCA - Observatoire de la Côte d'Azur, 06460 Caussols, France.

2. CNES - Centre National d'Etudes Spatiales, 34100 Toulouse, France.

Contact: Etienne.Samain@obs-azur.fr

Abstract

The new generation of optical time transfer T2L2 [1,2] (Time Transfer by Laser Link) has recently been accepted as a passenger of the Jason 2 satellite. The main objective of T2L2 on Jason2 is to compare remote clocks on earth. The project will also permit to follow-up from the ground, the on board clock of the DORIS[1] System. The performances expected are enhanced by one or two order of magnitudes as compared to existing microwave time transfer techniques, like GPS and TWSTFT[2]. After a description of the space instrumentation principle, we will present the metrological performances and give the current status of the project. Jason 2 will be launched in 2008 for a nominal mission duration of 3 years (5 expected) .

Introduction

The Time Transfer by Laser Link experiment (T2L2), initiated by OCA (Observatoire de la Côte d'Azur) and accepted by CNES (Centre National d'Etudes Spatiales), France, will be launched in mid-2008 on the altimetric satellite Jason 2. The experiment principle is issued from the classical laser telemetry techniques, with a specific instrumentation implemented onboard the satellite capable to tag the arrival time of laser pulses.

T2L2 history

T2L2 is the follow-on mission to LASSO (LAser Synchronization from Stationary Orbit) which was proposed in 1972 and launched in 1988 onboard the geostationary orbit satellite Meteosat P2. A first optical time transfer had successfully been achieved in 1992 between OCA, France and MacDonald, Texas [3]. This experiment measured a stability of 10^{-13} over 1000s and validated the feasibility of the concept. In 1996, a T2L2 instrument was proposed in the framework of the French PERSEUS mission to the Russian space station MIR, but the project was finally stopped at the end of the phase A. In the meantime it was accepted by ESA in the ACES (Atomic Clock Ensemble in Space) program scheduled on the International Space Station (ISS). T2L2 was one of the three scientific proposals of ACES, but had to be de-scoped in 2001 for some technical reasons concerning the whole ACES mission. Feasibility studies have been led by CNES and OCA for other flight opportunities (Myriade Micro-satellite, Galileo Test Bed), and finally a new opportunity appeared at the end of 2004, when NASA decided to abandon the WSOA instrument, an American contribution to the Jason-2 mission. A preliminary analysis confirmed the high interest to put a T2L2 instrument onto this altimetry-dedicated space vehicle and CNES decided to select the T2L2 instrument as a passenger on the Jason 2 mission.

[1] DORIS : Radio electric positioning system
[2] TWSTFT: Two-Way Satellite Time and Frequency Transfer

Principle and purpose of the experiment

T2L2 is an optical experiment that is able to establish a temporal link between remote clocks. The principle is based on the propagation of light pulses between laser stations and a satellite equipped with a specific instrumentation. The T2L2 payload is made with a photodetection device, a time-tagging unit, a clock (the DORIS ultra-stable oscillator (USO)) and a Laser Ranging Array (LRA). The ground station emits asynchronous laser pulses towards the satellite. LRA return a fraction of the received photons back to the station, while another fraction is detected and timed in the temporal reference frame of the onboard clock as (t_{board}). Each station records the start (t_{start}) and return (t_{return}) time each light pulse.

For a given light pulse emitted from station A, the synchronization χ_{AS} between the ground clock A and the satellite clock S is then derived from these data:

$$\chi_{AS} = \frac{t_{start} + t_{return}}{2} - t_{board} + \tau_{relativity} + \tau_{atmosphere} + \tau_{geometry} \quad (1)$$

$\tau_{relativity}$ is coming from relativistic effects, $\tau_{atmosphere}$ is the atmospheric delay and $\tau_{geometry}$ takes account of the geometrical offset between the reflection and detection equivalent points, depending on the relative position of the station and the satellite.

The same experiment can be lead from another station B and χ_{BS} can then be measured. The time transfer between A and B is then deduced from the difference between χ_{AS} and χ_{BS}. In a common view configuration, i.e. the two laser ranging stations are firing simultaneously towards the satellite, the noise of the onboard oscillator has to be considered over a very short time (time interval between consecutive pulses), so that it can be considered as negligible in the global error budget.

In a non-common view mode, the satellite local oscillator carries the temporal information over the distance separating laser stations. In the case of Jason 2 (driven by a quartz oscillator), we will have a significant degradation of the performances as soon as the time interval between passes is a few seconds (the maximum distance that allow this common view mode is roughly 7000 km). But in some cases, it will possible to keep a good time transfer performances even if the distance is greater than 7000 km by the use of intermediary laser stations located between station A and B. These stations will permit to build a virtual DORIS time scale from the clocks of each station.

Participation to the T2L2 experiment

The T2L2 ground segment is a laser station equipped with instrumentation to measure accurately both the start and return time of laser pulses. The laser station has to shoot with a 532 nm pulsed Nd:YAG laser having a pulse width between 10 to 200ps FWHM. The station can work between 10 Hz to a few Khz. Concerning the link budget, the conception of the space segment has been studied to detect low energy signals: the detection level onboard is comparable to the level in the ground. As a rule, if the ground station detects the impulse back, the same impulse should have been detected onboard as well.

Among the 40 laser stations in the world, 25 regularly range Jason 1 and will probably track Jason 2. Many laser stations have indicated their interest in participating to the T2L2 experiment (Figure 1).

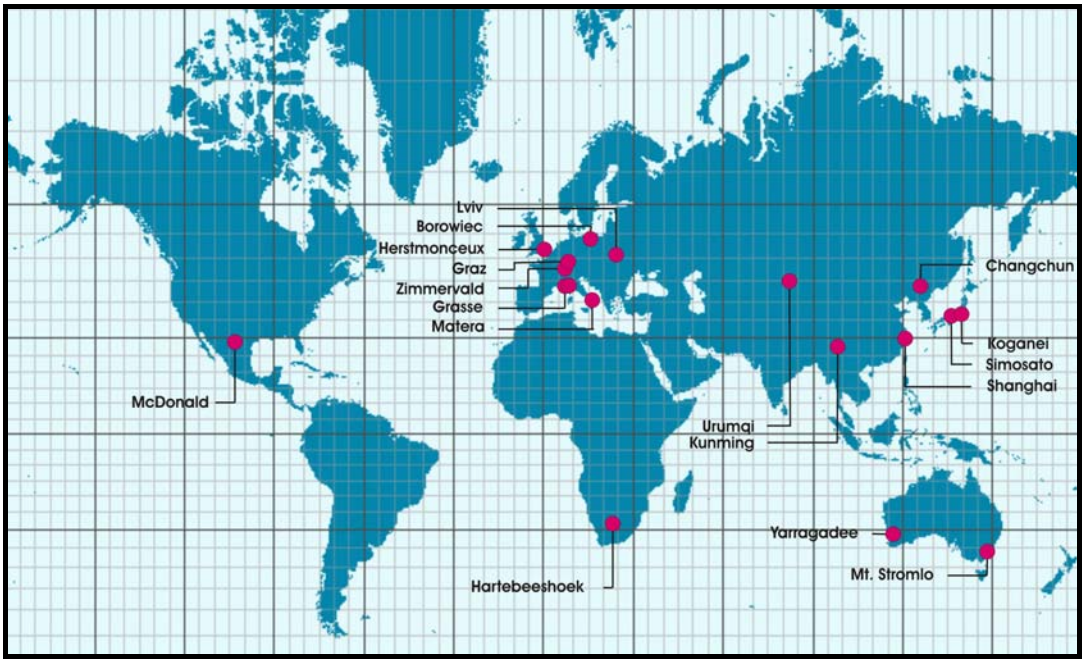

Figure 1: *T2L2 participation (October 2006)*

T2L2 on Jason 2

Jason 2 is a French-American follow-on mission to Jason 1 and Topex/Poseidon. Conducted by CNES and NASA, its goal is to study the internal structure and dynamics of ocean currents mainly by radar altimetry.

Jason 2 is build around a Proteus platform equipped with a dual-frequency radar altimeter Poseidon-3 and a microwave radiometer. For the needs of precise determination of the satellite orbit, three independent positioning systems are embarked: a Doris transponder, a GPS receiver and a LRA (Laser Ranging Array) target. The T2L2 instrument and two radiation studying payloads (Carmen-2, France and LPT, Japan) are supplementing the satellite instrumentation with some complementary objectives.

The satellite will be placed by a Delta launcher on the Jason 1's orbit at an altitude of 1,336 km and an inclination of 66°. This orbit allows common views at continental scale (about 7000 km baseline between stations). The time interval between two passes varies from 2 to 14 hours with an average duration of about 1000 s. The T2L2 specific instrumentation has a mass of 10 kg and a power consumption of 45 W. It includes (Figure 2):

- Two photo detection units located outside the main Jason 2 payload on the LRA boom (figure 3 right). Both are composed of avalanche photo detectors. The first one is working in a Geiger mode for precise chronometry[4,5] The other is in linear gain mode in order to trigger the whole detection chain and to measure the received optical energy and the reflected solar flux (earth albedo). To minimise the false detection rate, the detection threshold may be adjusted either by remote control or automatically as a function of the solar flux measurement.
- The electronic unit, located inside the Jason 2 payload module is composed of two main items (figure 3 right). The detection unit ensures the conversion of the laser pulse into an electronic signal and the event timer [6].

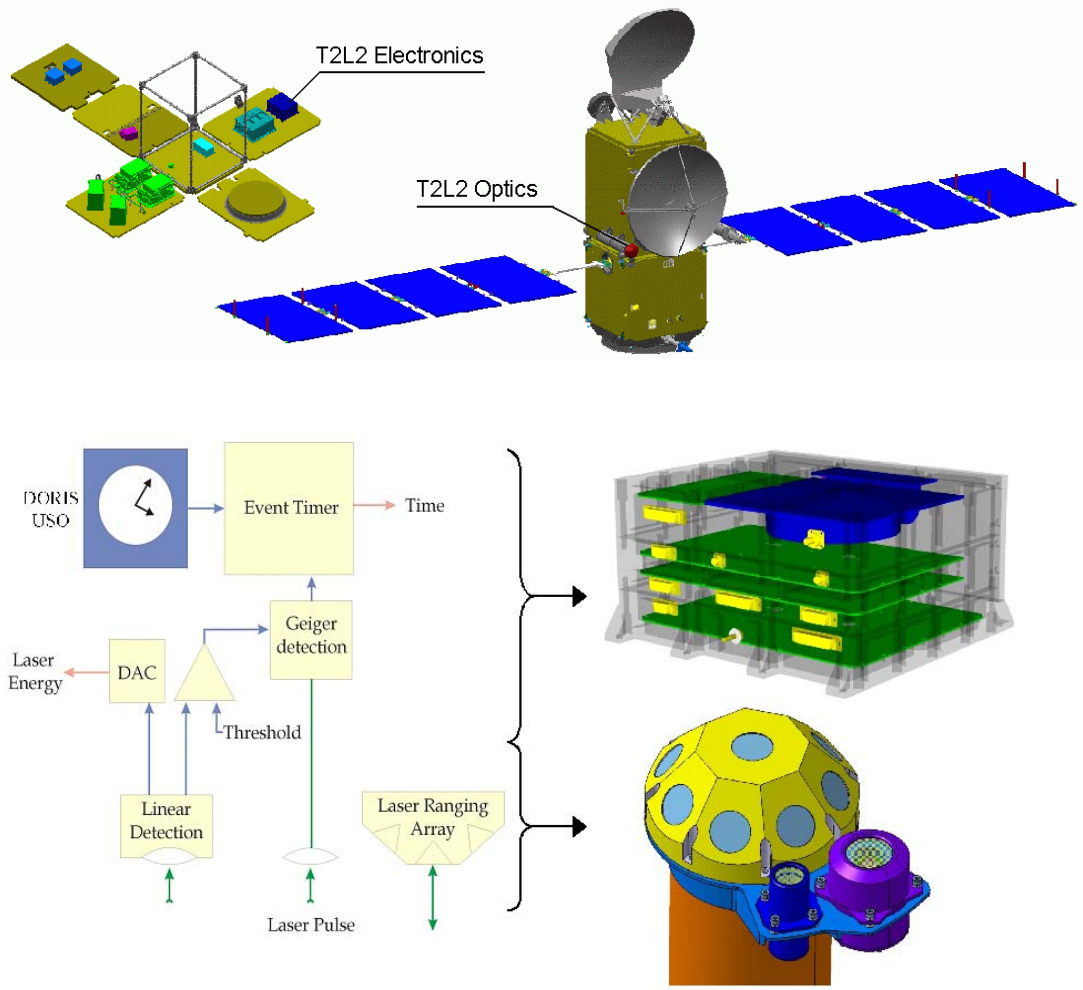

***Figure 2**: The integration of the T2L2 device inside the Jason-2 spacecraft*

Mission's objectives

The objectives of the T2L2 experiment on Jason 2 are threefold:

- Validation of optical time transfer, including the validation of the experiment, its time stability and accuracy. T2L2 will be a first step and a demonstration for future experiment based on one way laser ranging techniques in an interplanetary range: TIPO[3]. It should also allow the de-correlation of the effects coming from the target signature. In that way, it will permit to improve the precision of the telemetry.
- Scientific applications concerning time and frequency metrology allowing the calibration of radiofrequency time transfer (GPS and Two-Way), fundamental physics with the measurement of light speed anisotropy and alpha fine structure constant, Earth observation and very long baseline interferometry (VLBI).
- Characterization of the onboard Doris oscillator's drift, especially above the South Atlantic Anomaly (SAA) where the environment is highly irradiative. The two radiation instruments onboard will give the possibility to find a correlation between the expected and measured drift and propose adequate corrections.

Performance budget

T2L2 has ground-ground time transfer accuracy better than 100 ps. This will allow inter calibration between different time transfer methods by extracting the error

[3] TIPO: *Télémétrie InterPlanétaire Optique* / Optical InterPlanetary Telemetry

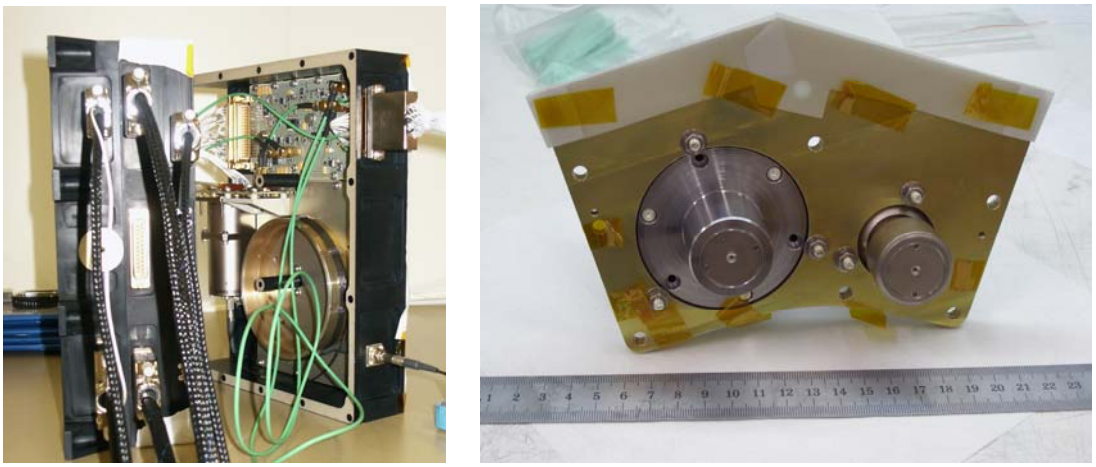

Figure 3: *Left : electronic of the flight model. The cylinder on the right side, support an multi mode optical fiber that generate a delay between the 2 photo detection. Right: the photo detection module (linear photo detector on the left side)*

caused by the transfer techniques themselves. T2L2 is particularly interesting to calibrate the regular time transfer used for the construction of international time scales (TAI) in particular the "Two-Way" (TWSTFT) that is about to become the quality reference for these scales. T2L2 will also permit to validate and to qualify the time transfers of Two-Way phase or GPS phase.

In term of stability, the comparison of T2L2 with the existing microwave links is shown on Figure 4. In a common view configuration (red bottom curve), the stability is better than 1 ps over an integration of 1,000 s. In non-common view, when conditions will not permit to build a virtual DORIS time scale, T2L2 will still offer an interesting alternative for radiofrequency calibration campaigns.

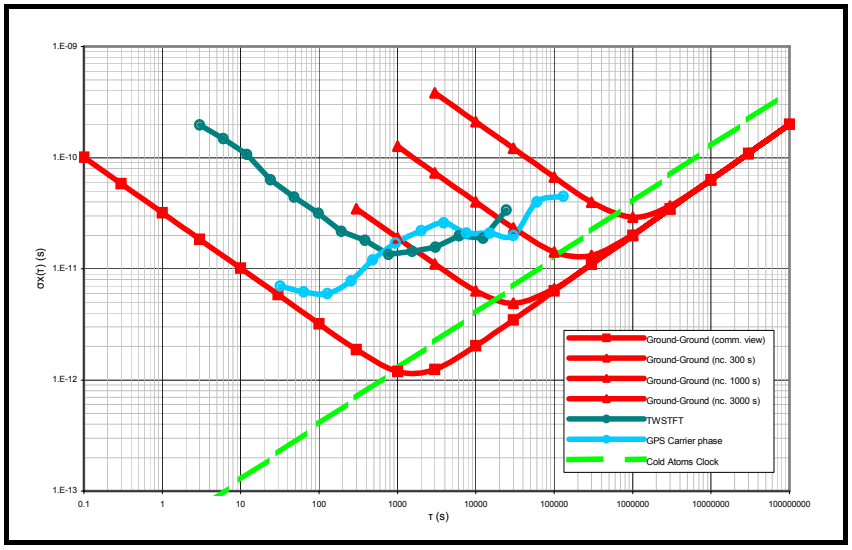

Figure 4: *T2L2 stability in common and non-common view configuration in* $\sqrt{\text{TVAR}}$

Current Status

The decision to put the T2L2 instrument in the Jason-2 satellite was taken on July 2005. The phase B started in September 2005 and entered in phase C/D in January 2006. Only one proto-flight model was built for the optics, while the electronics was developed in three steps: prototype boards, engineering model (EM) and flight model (FM). Metrological tests on EM have been done in July 2006. The flight model is now

fully integrated and the qualification processes is running now. The delivery of the instrument for the integration on the Jason 2 satellite is expected in April 2007.

A test bed has been developed at OCA to evaluate the metrological performances of the T2L2 space instrument and to perform some calibrations of both electronics and optics. This test bed will precisely reproduce the experimental conditions that will meet in orbit. The optical subsystem of the test bed was designed to simulate laser stations by illuminating the optics with faint laser pulses and also background illumination. The T2L2 photo detection module is mounted on 2 axes gimbals able to emulate the attitudes of the satellite in the range of ±60°. A high performance timing system is used as a timing reference. The experimental setup also includes a DORIS space clock engineering model in order to simulate the conditions on the satellite Jason 2, and alternatively a Cesium standard for time accuracy measurements. The tests that were so far conducted on the engineering model show the compliance with the metrology specifications for both the photo detection and the event timer.

Conclusion

With an improvement of one order of magnitude as compared to microwave time transfer techniques, T2L2 will give the possibility to compare cold atoms clocks at a level never reached before. It will allow the calibration of the existing radiofrequency links like GPS and TWSTFT with an improvement of at least one order of magnitude. T2L2 will also allow the precise characterization of the DORIS USO onboard Jason 2. The validation of the time and frequency transfer in space by T2L2 will represent an important step for further missions using this kind of technology, especially in a one-way mode in the solar system [7,8]. Jason 2 will be launched mid-2008 for a nominal duration of 3 years.

References

[1] Fridelance, P., E. Samain and C. Veillet, "Time Tranfer by Laser Link: a new optical time transfer generation", Experimental Astronomy 7, 191, (1997)

[2] Samain, E., J. Weick, P. Vrancken, F. Para, D. Albanese, J. Paris, J.-M. Torre, C. Zhao, Ph. Guillemot and I. Petitbon, "Time Transfer by Laser Link: The T2L2 Experiment on Jason 2 and further Experiments", Int. Journal of Modern Phys. D, World Sci. Publ. Company, (2007), (in press)

[3] P. Fridelance, C. Veillet, "*Operation and data analysis in the LASSO experiment*", Metrologia, 32, 27-33, 1995

[4] I. Procazka , K. Hamal, "*Recent achievements in solid state detector technology for laser ranging*", 2 , 469, Proceedings of the 9th International Workshop on laser ranging instrumentation, 1994

[5] E. Samain , "*Timing of optical pulses by photodiode in Geiger mode*", Applied Optics, 37, No 3, pp 502-506, 1998.

[6] Samain, E. et al, OCA Event Timer , this proceedings 2006.

[7] E. Samain, One way laser ranging in the solar system, the TIPO Project (Télémétrie InterPlanétaire Optique), EGS, 2002.

[8] Wei-Tou Ni, Proceedings of the first International ASTROD symposium on laser astrodynamics, space test of relativity and gravitational – Wave astronomy, International journal of modern physics, 2002.

New Application for Khz Laser Ranging: Time Transfer Via Ajisai

Toshimichi Otsubo[1], Hiroo Kunimori[2] and Tadahiro Gotoh[2]

1. Kashima Space Research Center, National Institute of Information and Communications Technology, 893-1 Hirai, Kashima 314-8501 Japan
2. Koganei Headquarters, National Institute of Information and Communications Technology, 4-2-1 Nukui-kita, Koganei 184-8795 Japan

Contact: otsubo@nict.go.jp / FAX : +81-299-84-7160

Introduction

It was 14 years ago when the use of laser ranging technique was proposed for time transfer application for the first time (Kunimori, et al., 1992). The concept is to exchange laser pulses between two laser ranging stations via the curved mirrors carried on the AJISAI satellite (Sasaki and Hashimoto, 1987) shown in Fig. 1. The AJISAI satellite, launched in August 1996, carries 314 mirror panels as well as 1436 retroreflectors. Laser ranging stations usually detect retroreflected signals from the retroreflectors. However, the optical reflection by the mirrors were expected to be useful as if they were a two-way 'zero-delay' optical transponder, although they were originally designed to be used for photographical observations. It should be also emphasised that the optical components on the AJISAI satellite has almost no limit of lifetime, and therefore it can be used for many decades with no risk factors for long-term variation of transponder delay, etc.

This concept has not been realised yet. In this paper, the difficulties we have encountered for the realisation of this concept are briefly reviewed. Then, some new possible approaches, especially the use of the kHz laser ranging technology, are proposed. A possible scenario is lastly given based on the assumption of multiple kHz laser ranging station in Europe region (Kirchner and Koidl, 2004; Gibbs, et al., 2006).

Time Transfer via AJISAI: Concept and Difficulties

As seen in Fig. 1, the surface of the AJISAI satellite is mostly covered by the mirrors whose curvature is 8.5 to 9 metres. The size of each mirror panel is approximately 400 cm2 (~ 20 cm by 20 cm) at maximum. The laser retroreflectors (12 retroreflectors in one holder) are placed in the gap of the mirror panels.

This satellite flashes three or six times per its rotation period when it is illuminated by the sun. This is because three mirror panels located in the same row point toward the same latitudal angle. The placement of mirror panels was arranged so that the flashed mirror panels can be identified by the time intervals between flashes.

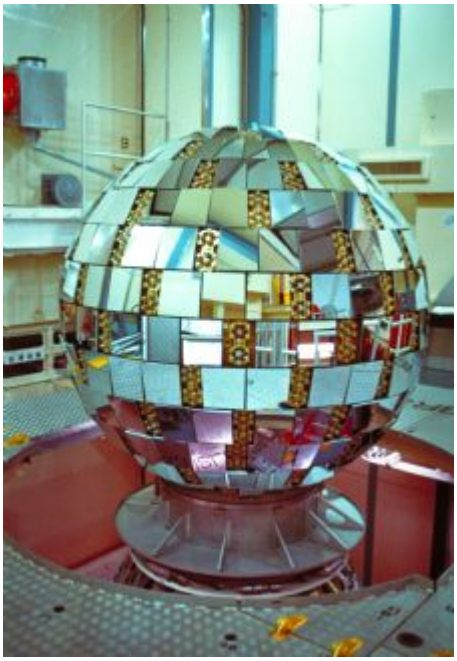

Figure. 1. *Japanese geodetic satellite AJISAI (photo: courtesy of JAXA).*

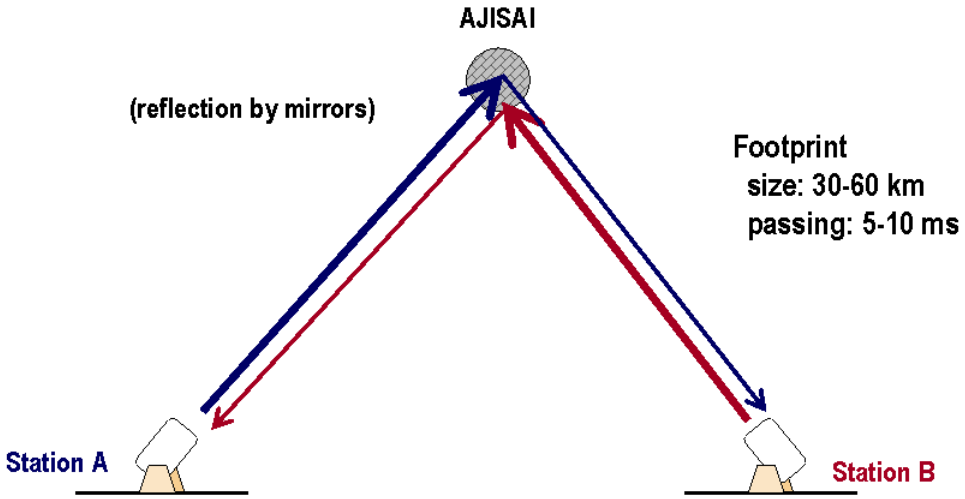

Figure 2. *AJISAI time transfer experiment: basic concept.*

A schematic view of the time transfer experiment via AJISAI proposed by Kunimori et al. (1992) is shown in Fig. 2. Like the radio-based two-way time transfer, the signal transmitted from one station goes to the other and vice versa. The curved mirrors make the reflection beam much wider to about 30 to 60 km size. Such a large footprint passes the receiving station just in 5 or 10 milliseconds.

The time diagram of signal passage between station A and B is illustrated in Fig. 3 where the 'ordinary' ranging of the station A and the signal transfer from the station A to the station B are shown. The signal transfer from the station B to the station A is simply given just by swapping the subscripts A and B. The case [1] is the prediction where the distance (in a time unit) R_{A1}* is the predicted one-way distance from the station A to the satellite and the time duration D_{A1}* is the predicted one-way internal system delay. The laser pulse is intended to hit the satellite at epoch t_0 of an imaginary 'true' clock. Assuming the clock of the station A is fast by ΔT_A compared to the 'true' clock, the station-transmission and the satellite-hit events come earlier by ΔT_A (case [2]). In reality, the laser does not exactly fire at the commanded epoch, and the delay is hereby set to L_A (case [3]). Now the start event $t_T(A)$ is given as:

$$t_T(A) = t_0 - \Delta T_A - R_{A1}^{*} - D_{A1}^{*} + L_A \quad \text{('true' clock)}$$
$$= t_0 - R_{A1}^{*} - D_{A1}^{*} + L_A \quad \text{(station A's clock)}$$

Then, neglecting the centre-of-mass correction of the satellite, the reflected signal by retroreflectors comes back to the station A at:

$$t_R(A \to A) = t_0 - \Delta T_A + R_{A2} + (R_{A1} - R_{A1}^{*}) + D_{A2} + (D_{A1} - D_{A1}^{*}) + L_A \quad \text{('true' clock)}$$
$$= t_0 + R_{A2} + (R_{A1} - R_{A1}^{*}) + D_{A2} + (D_{A1} - D_{A1}^{*}) + L_A \quad \text{(station A's clock)}$$

where R_{A1} and R_{A2} are the true outgoing and incoming one-way distance and D_{A1} and D_{A2} are the true outgoing and incoming one-way internal system delay.

What we usually use for the laser ranging is the difference (time interval) of the above two:

$$t_R(A \to A) - t_T(A) = R_{A1} + R_{A2} + D_{A1} + D_{A2}$$

from which we subtract the internal system delay D_{A1} +D_{A2} to obtain the two-way distance R_{A1} +R_{A2}. The clock offset ΔT_A and the laser firing delay L_A does not appear here, and therefore they are hardly observable from the ordinary laser ranging measurement.

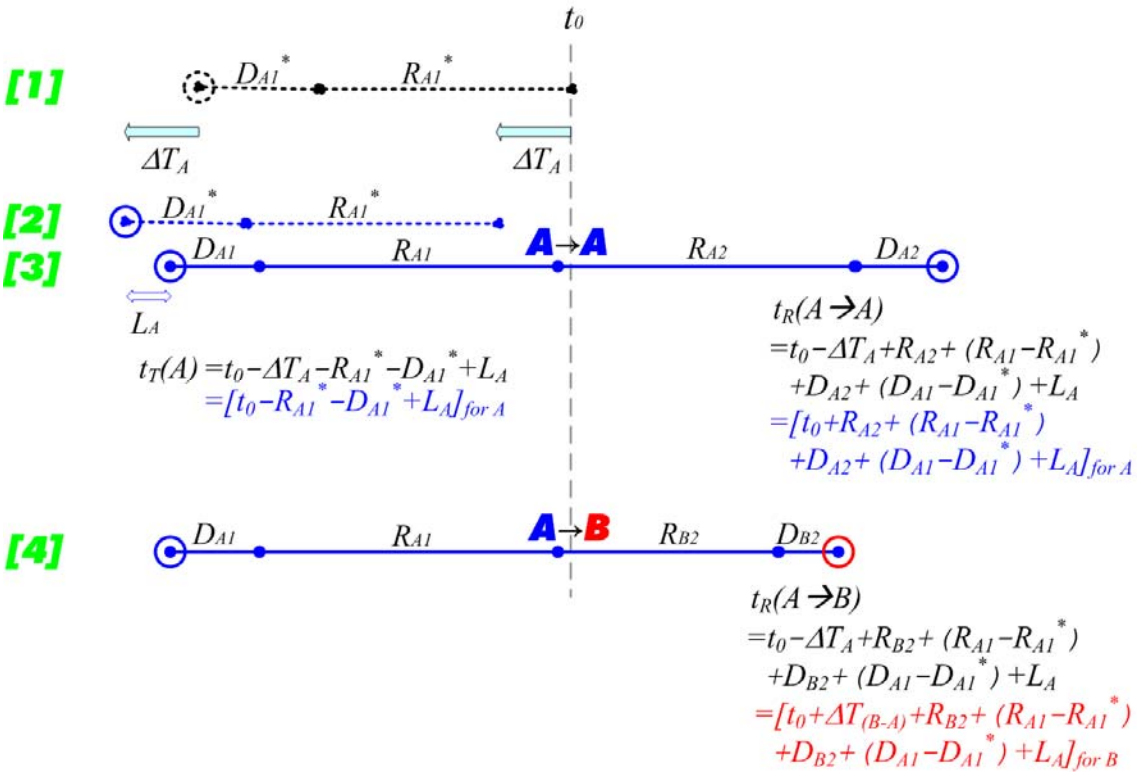

Figure 3. *Time diagram of ordinary laser ranging (A→A) and time transfer (A→B).*

Coming back to Fig. 3, the case [4] shows the signal transfer from the station A to the station B. The stop event at the station B comes at:

$$t_R(A \to B) = t_0 - \Delta T_A + R_{B2} + (R_{A1} - R_{A1}^*) + D_{B2} + (D_{A1} - D_{A1}^*) + L_A \quad \text{('true' clock)}$$
$$= t_0 + \Delta T_{B-A} + R_{B2} + (R_{A1} - R_{A1}^*) + D_{B2} + (D_{A1} - D_{A1}^*) + L_A$$
(station B's clock)

where the subscript B corresponds to variables for the station B. The opposite direction from the station B to the station A is given by an equation of swapping A and B in the above formulae. Using them, the two-way time transfer to obtain the difference of the clock offset, $\Delta T_{B\text{-}A} = \Delta T_B - \Delta T_A$ is given as the difference of two range observations $\rho_{A\text{->}B}$ and $\rho_{B\text{->}A}$, as below:

$$\rho_{A\to B} - \rho_{B\to A}$$
$$= t_R(A \to B) - t_T(A) - t_R(B \to A) + t_T(B)$$
$$\vdots$$
$$= 2\Delta T_{B-A} + [(R_{B2} - R_{B1}) - (R_{A2} - R_{A1})] + D_{B2} - D_{B1} - D_{A2} + D_{A1}$$

Now the double-difference $[(R_{B2} - R_{B1}) - (R_{A2} - R_{A1})]$ can be precisely calculated from the orbital motion of the satellite. On the other hand, the double-difference of the incoming/outgoing one-way internal system delay should be given to obtain the absolute value of $\Delta T_{B\text{-}A}$. That is, either (1) incoming minus outgoing ($D_{A1} - D_{A2}$) and ($D_{B1} - D_{B2}$) should be given, or (2) inter-station difference of one-way internal system delay ($D_{B1} - D_{A1}$) and ($D_{B2} - D_{A2}$) should be given. These values cannot be easily measured from the ordinary laser ranging systems. Note that, in spite of the difficulties in deriving the absolute accurate $\Delta T_{B\text{-}A}$, the variation of clock offsets would be relatively easily observed, leaving the constant offset of the '*D*' values and assuming them to be constant.

Beside this issue, the experiment itself has seemed unrealistic due to the following problems:

(a) The footprint passage time duration is just 5 to 10 ms. Compared to the laser firing interval of 100 to 200 ms (5 to 10 Hz lasers), it is much shorter. The footprint passage happens usually only three times per the rotation period of AJISAI, currently ~ 2s. Hence, the probability of hitting the laser at the right time was just 2.5 to 10 %. The chance was very limited.

(b) The mirror-reflection signal should reach the other station. If one wants to use a single range gate (common to laser ranging observation), the signals from the station A and the station B should hit the satellite almost at the same time. The multiple stop events should also be recorded, which is not possible by the ordinary time interval counters.

(c) The expected number of photons was just 1 to a few photons for the mirror-reflection signals, assuming a 100mJ/pulse laser. Very high sensitivity (or very strong laser) was required.

Expected breakthrough using kHz laser ranging technology

The problems (a) and (b) in the previous section are likely to be solved by the newly emerging kHz laser ranging networks. Firstly, as for the problem (a), the kHz laser (2 kHz in this case) fires 10 to 20 times per the footprint passage duration. The observation opportunity will not be missed. The kHz laser ranging systems almost automatically requires an event timer, instead of a time interval counter, due to the longer satellite ranges compared to the laser firing interval. The problem (b) will also be solved.

Especially in the European laser ranging network, multiple stations are moving toward the kHz laser ranging, following a very successful achievement at Graz, Austria. This region might be useful to exchange time signals via AJISAI between ~1000 km distant stations.

On the other hand, the link budget issue (the problem (c) in the previous section) gets more serious with kHz lasers. For instance the laser energy transmitted from the Graz system is 400 μJ/pulse, which is only 0.4 % of a traditional 100 mJ/pulse laser. The expected number of photons becomes a few hundredths of photons/pulse, and 1/10 to 1 photons/footprint passage. This would probably be the key issue for the realization of this experiment. We need to increase the laser energy and/or enhance the optical efficiency.

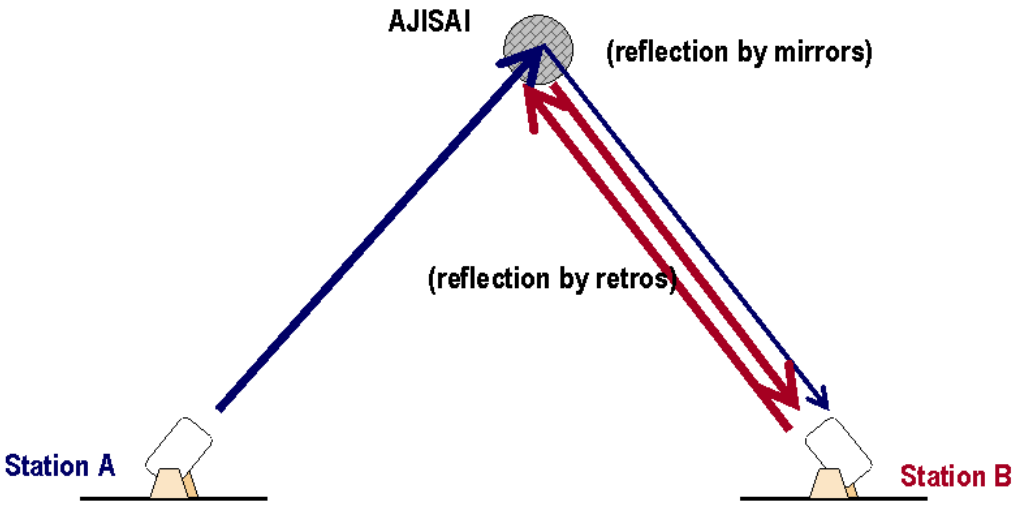

Figure 4. *AJISAI time transfer experiment: new concept.*

New experiment algorithms

As the single (A→B or B→A) signal transfer itself seems an uneasy task due to the weak link, we cannot expect the two-way (A→B and B→A) signal transfer at least at the initial stage. We re-examined the time diagram (Fig. 3) and conceived a novel way to achieve the time comparison experiment, as follows.

Let us assume the situation illustrated in Fig. 4, that is, one gets the single (A→B) signal transfer and the laser ranging (B→B). Subtracting the former range observation $\rho_{A->B}$ by the latter range observation $\rho_{B->B}$:

$$\begin{aligned}
&\rho_{A\to B} - \rho_{B\to B} \\
&= t_R(A \to B) - t_T(A) - t_R(B \to B) + t_T(B) \\
&\quad \vdots \\
&= \Delta T_{B-A} + [R_{A1} - R_{B1}] + [D_{A1} - D_{B1}]
\end{aligned}$$

where the clock offset difference $\Delta T_{B\text{-}A}$ appears. The second term, one-way range difference $[R_{A1} - R_{B1}]$, can be given at a few cm precision from an orbit determination procedure. The centre-of-mass corrections for R_{A1} and R_{B1} are different in this case due to the different reflection point: a mirror and retroreflectors, which should be taken into account for sub-nanosecond time comparison. The third term, difference of one-way outgoing system delay $[D_{A1} - D_{B1}]$, is still a problem to be solved, like the case of the two-way signal transfer. It is, nevertheless, now a difference of outgoing system delay, not the double difference of outgoing and incoming system delay.

Likewise, for example, by subtracting $\rho_{A->B}$ by $\rho_{A->A}$, the outgoing path will be cancelled and the incoming differences should be considered.

In this way, the clock offset information can be obtained by the single signal transfer and the ordinary laser ranging observation. This will ease the difficulties, especially on the weak link budget.

Conclusions

The time transfer via AJISAI is a long-lasting technology potentially with a very high precision/accuracy of 100 ps or even better. This will be one of new fields for a newly emerging kHz laser ranging 'network', especially in Europe. We have also derived a new algorithm which requires only single signal transfer, which will ease the weak link problem.

References

[1] Kunimori, H., F. Takahashi, T. Itabe, A. Yamamoto, "Laser ranging application to time transfer using geodetic satellite and to other Japanese space programs," Proc. 8th International Workshop on Laser Ranging Instrumentation, 1-34—1-42, 1992.

[2] Sasaki, M. and H. Hashimoto, "Launch and observation program of the experimental geodetic satellite of Japan," IEEE Trans. Geoscience and Remote Sensing, GE-25, 5, 526-533, 1987.

[3] Kirchner, G. and F. Koidl, "Graz KHz SLR System: Design, Experiences and Results," Proc. 14th International Workshop on Laser Ranging, 501-505, 2004.

[4] Gibbs, P., C. Potter, R. Sherwood, M. Wilkinson, D. Benham, V. Smith, "Some Early Results of Kilohertz Laser Ranging at Herstmonceux," in these proceedings, 2006.

A Satellite Tracking Demonstration on Ground Using a 100mm Aperture Optical Antenna for Space Laser Communication

H. Kunimori[1], M.Okawa[1], H.Watanabe[1], Y. Yasuda[2]

1. National Institute of Information and Communications Technology
2. Emeritus Waseda University, Japan
Contact: kuni@nict.go.jp , 4-2-1 Nukui-kita, Koganei 184-8795 Japan

Abstract

The Next Generation LEO System (NeLS) optical terminal was designed for 1.5um wavelength and 2Gbps data rate communication between 500 km – 3000 km inter-satellite link. In the course of ground validation test, using Coarse Pointing Mechanism and Optical Antenna, we demonstrated open tracking capability by ranging to a satellite AJISAI.

Introduction

Figure 1: *Concept of NeLS: Next Generation LEO System*

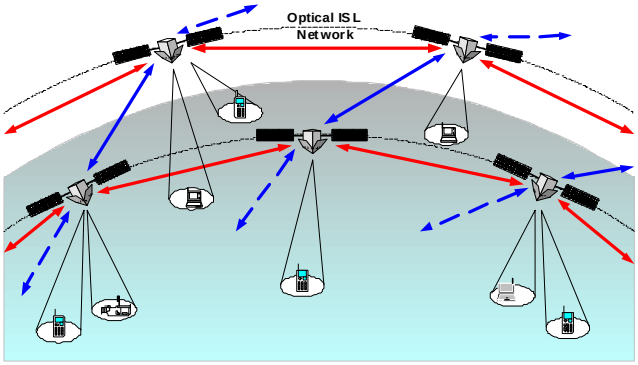

The Next Generation LEO System Research Center (NeLS) in National Institute of Information and Communications Technology (NICT), of Japan, formed in 1997 for the key technology development of space communication network in future [1,2]. Fig. 1 and Fig. 2 show a concept and development schedule for optical communication part, respectively. Since 2002, it has focusing on the development of optical inter-satellite link technology for the future communication demanding a high data transmission for global multimedia service, as well as requirement of earth observation/ science data communication to ground.

Optical terminal and key components

Figure 2: *NeLS Optcal Engineering Model Development Schedule*

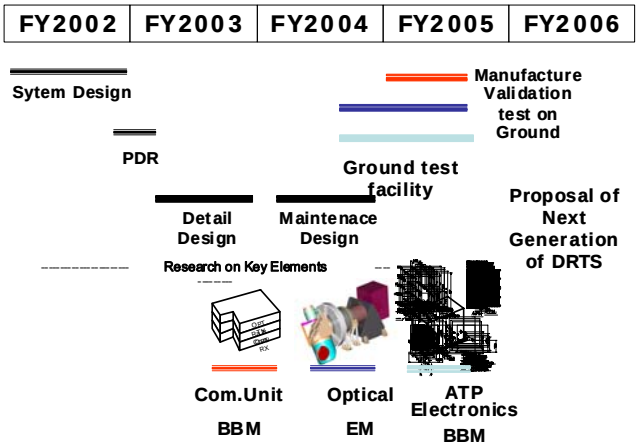

Fig. 3 shows block diagram of optical terminal. The optical terminal consists of four units, namely 1) Coarse Pointing Mechanism (CPM) located outside the spacecraft on mission panel, 2) Optical Antenna (OANT) as one of fixed part of optics located on mission panel 3) AT&P unit located outside the spacecraft, and 4) Communication Unit which interface both transmit & receive by optical fibers, located inside the spacecraft.

Figure 3: *NeLS Optical Terminal*

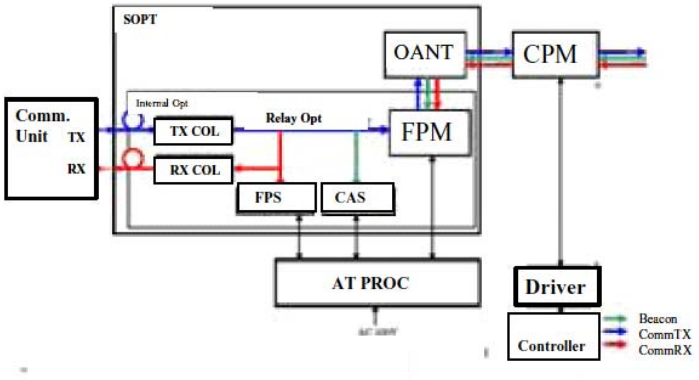

Figure 4: *A 10cm class Coarse Pointing Mechanizm (CPM)*

Item	Specification
Range of drive axis	Az:+/-275deg EL:+/-110deg
Maximum drive speed	3.0deg(slew) 1.0deg(track
Effective aperture size	85mm
Resolution of encorders	2/10000deg
Weight	16kg

CPM utilizes two-flat mirror type 2-axis gimbals (shown in Fig.4 picture and specification) so-called elbow-type has been adopted to cover all direction in space, where optical antenna fixed to satellite body.

In addition to OANT, as a fixed part of optics, a wide range Fine Pointing Mechanism (FPM), a Coarse Acquisition Sensor (CAS), a Fine Pointing Sensor (FPS), a Transmitting Collimator (TX COL), and a Receiving Collimator (RX COL) are integrated onto an optical bench with relay optics. AT&P UNIT includes terminal control processor circuit and power supply.

The Optical Antenna shown in Fig.5 has type of Cassegrain, where secondary mirror is supported by tripod and main reflector diameter of 125mm diameter, made by material of SiC with gold coating. Total effective focal length is 2600mm and magnification is about 20.

Other key components of internal optics include a fine pointing mirror made by voice coil actuators and GAP sensors, and transmitting and receiving fiber couplers has been tested as space qualification devices(Fig.6).

Figure5: *Subsystem - OPTICAL ANTENNA*

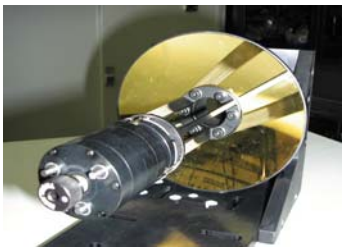

Figure 6: *Key components of internal optics*

Fine Pointing Mirror (FPM)

Transmitting Fiber Coupler (left)
Receiving Fiber Coupler& QD (right)

Utilities for ground test

To perform functional test and validation of optical terminal, we have developed one of utilities an optical tracking simulators utilized in a room spacing several meters between optical terminal and target

Figure 7: *Optical Tracking Simulator for ground experiment*

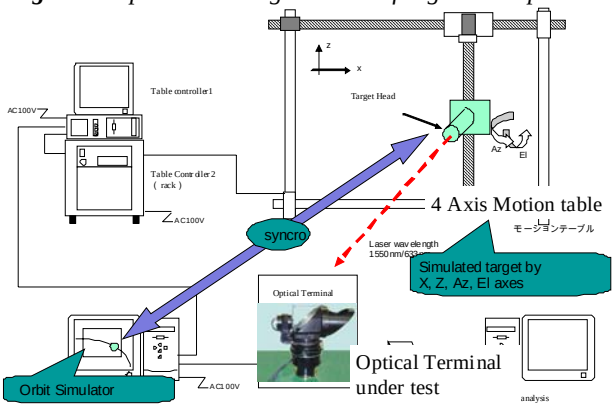

antenna. The target has on 4 axes (X-Z, Tip/Tilt) movement platform and has optical INPUT/OUTPUT capability. Fig.7 shows a schematic configuration of optical tracking simulator. The movement is programmed based on orbit simulation. Although the optical characteristics of terminal is different from that of far field, a basic function of acquisition and tracking during communication has been tested and 2.5Gbps communication BER data acquired and application of HDTV was demonstrated.

Another utility for optical terminal on ground outside, air-conditioned enclosed dome with a 30cm diameter optical window has been developed (Fig.8). The dome has axis of azimuth and rotor on azimuth structure made of stainless steel. The dome is on a box with 2 x 1 x 1 meters dimension, in which there is optical table set as vibration isolated manner, carrying optics and mechanics. Under table there are room and also carrying drivers of dome and electronics and power supply for optical terminal.

Fig.9 shows a schematic view of arrangement in a dome box called MML (Micro Mobile Laser) utility box. It also has optics for satellite laser ranging set that sharing beam through CPM by 45 degrees flat mirror.

Satellite Pointing capability test

Figure 8: *Utility development for Ground outside experiment*

The CPM was set up on optical bench so that mechanical & optical axis is aligned to gravity field (i.e. leveling) and other principal axis of equipments (laser and receivers). Two axis intersection angle offset orthogonality was measured as 80 ± 5 arcseconds. And star calibration of axis resulted in several arcseconds rms after rigorous alignment work done. Fig.10 shows a follow-on error when CPM tracking a Starlette satellite simulation pass which maximum elevation of 85 degrees. Two passes consecutively run shown. Since keyhole effect exists at zenith on Alt/Az axis gimbals, the performance of Az axis about maximum elevation was degraded to 10 arcseconds, however most of errors except key hole was within one arcsecond. Elevation axis has the same characteristics, but mean following error was larger (2 arcseconds rms) than that of Azimuth. Using standard SLR equipment with a nano second pulse width and 20mJ/pulse Nd:YAG lasers set up on table. We have performed laser ranging to a satellite AJISAI. Return proves the tracking system as open loop (means no use of beacon from satellite) working. Fig.11

Figure 9: *Configuration of Optical comm. and SLR equipments*

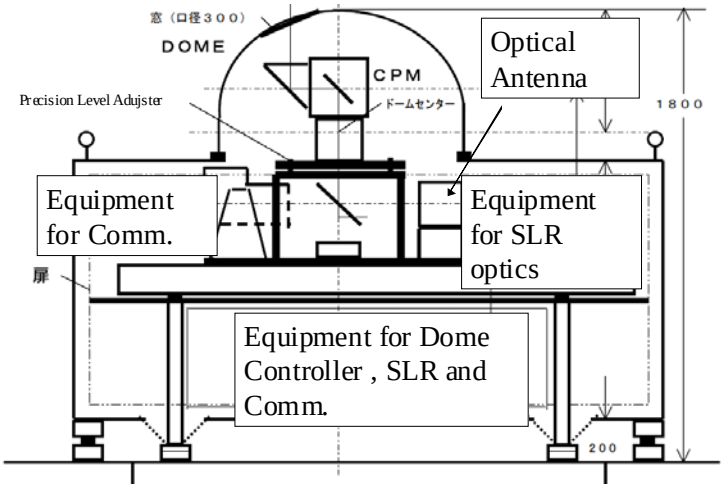

shows range residual vs observation time and there is a series of dots among dark noise and background noises that is from satellite returns. Fig.11 shows range residual vs observation time and there is a series of dots among dark noise and background noises that is from satellite returns.

We have had such four passes acquiring satellite returns during two weeks campaign. During campaign ranging to fix target to a 20meters to 4km distance was used as calibration of range as well as beam divergence and direction. The location of 4km distance is used as fixed distance communication experiment being done almost paralleled.

Figure 10: *LEO Tracking follow-on error evaluation of CPM by Starlette 85 deg elevation pass*

Black dot: Following Error Axis range+- 15arcsec
Red dot error RMS(2sec avarage) Axis range 0-10arcsec

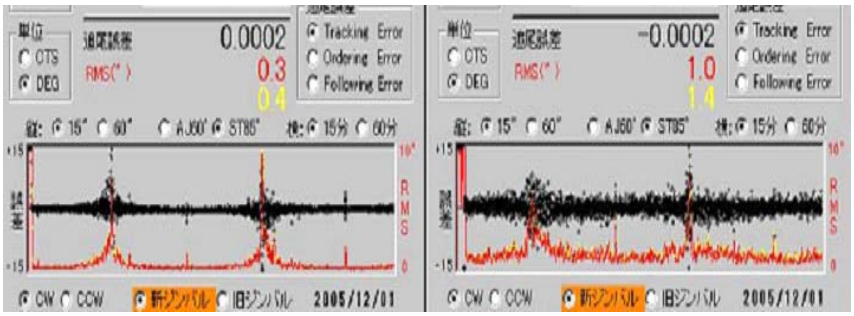

AZ axis:
<1arcsec rms except around zenith about 10arcsec rms

EL axis:
< 2arcsec rms except around zenith about 6 arcsec rms

Summary

The Next Generation Inter-satellite Laser Communication Terminal Optical Part Engineering Model has been developed. By using newly developed utility for ground

test validation, such as 4 axis motion table, mobile dome, optical terminal for 1.5um wavelength and 2.4Gbps data rate was evaluated in near-field (5m-5km) including ATP performance with atmospheric existence. Using Coarse Pointing Mechanism (CPM) and 10 cm class Optical antenna and, and associated 532nm pulse laser connection pass, we have demonstrated open-loop satellite tracking capability by ranging to AJISAI. Next Step is now using evaluation of those, we are proposing the next generation of DRTS (Data Relay Technology Satellite) in early 2010's

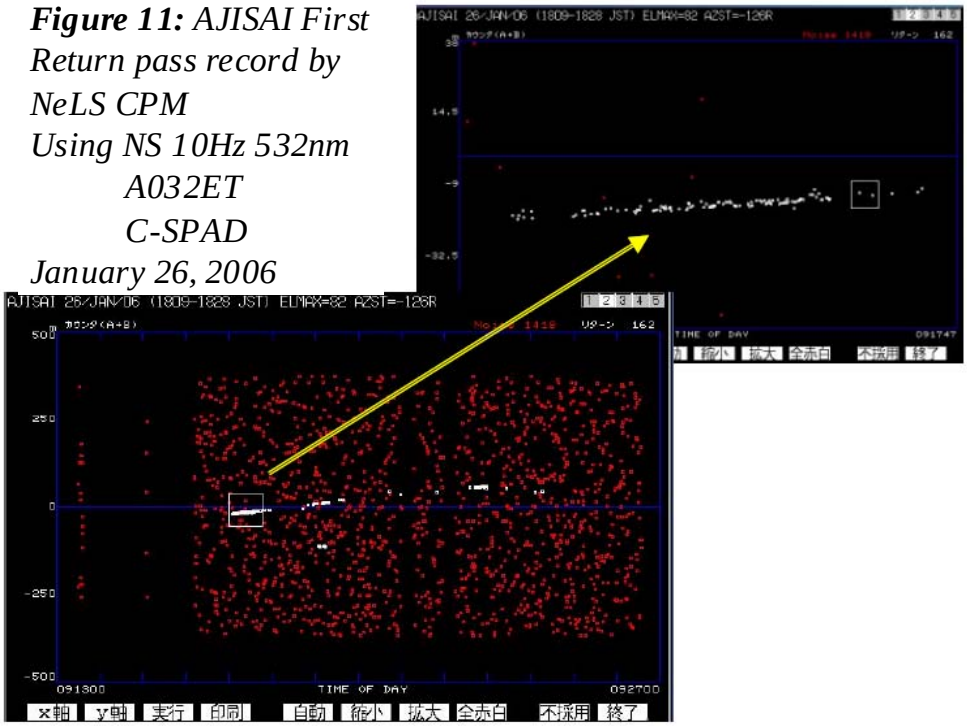

Figure 11: *AJISAI First Return pass record by NeLS CPM*
Using NS 10Hz 532nm
A032ET
C-SPAD
January 26, 2006

Acknowledgement

Authors would like to special thanks to who support the NeLS ground-satellite test experiment, namely N.Endo (INDECO), T.Yamaguchi (DENOH), Y.Suzaki (UNIVERSE), A.Hasegawa (SHOTOKU) and J.Guilfoyle (MTP).

References

[1] E. Morikawa, et.al, "R&D of A Next Generation LEO System for Global Multimedia Mobile Satellite Communications", 53th International Astronautical Congress, IAC-02-M.4.02, Huston US, 10-19 Oct. 2002.

[2] Y. Koyama, et.al., " Optical terminal for NeLS in-orbit demonstration", Proc.SPIE .Vo.5338, pp29-36., Jan.2005.

The NASA Satellite Laser Ranging Network: Current Status and Future Plans

David L. Carter[1]

1. NASA Goddard Space Flight Center, Code 453, Greenbelt, Maryland, USA 20771

Abstract

Over the past few years, the NASA Satellite Laser Ranging (SLR) Program has experience a resurgence of energy. In preparation for the completion and deployment of the SLR 2000 Replacement Systems, the NASA heritage SLR network continues to provide quality SLR data products to the International Laser Ranging Service (ILRS). Recently, NASA made the decision to return two critical stations in Maui, Hawaii and Arequipa, Peru back to operational status. NASA has been working hard to bring these two stations back on-line with the replacement of the HOLLAS station with the TLRS-4 system and the re-start of the TLRS-3 system. Other highlights have occurred throughout the NASA SLR network. The current status and the future plans of the NASA SLR Network will be discussed in this paper.

Background

The NASA SLR network consists of eight stations. NASA built five trailer-based Mobile Laser Ranging Stations (MOBLAS) and two highly compact Transportable Laser Ranging Systems (TLRS). The University of Hawaii and the University of Texas have operated two high performing Observatory SLR systems at their respective Universities. The University of Texas system has Lunar Laser Ranging (LLR) capability. NASA also has partnerships with foreign Government agencies and Universities for the operations and maintenance of MOBLAS systems. Under these partnerships, NASA continues to provide the SLR system, training, engineering support, and spare parts to maintain operations. The host country provides the site, local infrastructure, and the operating crew.

In February 2004, a forty percent decrease in the NASA SLR budget caused major reductions to the NASA SLR Network. The reductions included reduced network infrastructure, operational coverage at the stations, sustaining engineering staff, and data operational support. The MOBLAS-7 (Greenbelt, Maryland), McDonald Laser Ranging System (MLRS) (Fort Davis, Texas), and HOLLAS (Maui, Hawaii) stations were reduced to one shift operations. The NASA operator was removed from MOBLAS-8 site in Tahiti. In addition, the TLRS-3 site in Arequipa, Peru closed in February 2004, and the HOLLAS site in Maui, Hawaii closed in June 2004.

Resurgence of NASA SLR Network

In October 2004, the NASA SLR program experienced a resurgence of energy. Additional funding was provided by NASA Headquarters to re-open the TLRS-3 system in Arequipa, Peru. The TLRS-4 system, which was in caretaker status at Goddard Space Flight Center, was returned to operational status and shipped to Maui to replace the HOLLAS station. Another operational shift was added to the MLRS in Fort Davis, Texas. Additional highlights occurred throughout the NASA SLR network which are listed below.

MOBLAS-4 (Monument Peak, California):

NASA continued its collaboration with HTSI for the operations and maintenance of the MOBLAS-4 system. The site installed new Geoscience equipment. A Doppler Orbitography and Radiopositioning Integrated by Satellite (DORIS) instrument and a seismic instrument were installed at the SLR site. The DORIS instrument is from the Institut Geographique National (IGN) in France and the seismic instrument is from SCRIPPS Institution of Oceanography in San Diego, California. The site also installed a newly High Performance forWireless Research and Education Network (HPWREN) high speed internet access. The station is continuing three shift operations, five days per week, twenty-four hours per day.

MOBLAS-5 (Yarragadee, Australia):

NASA continued its collaboration with Geoscience Australia (GA) for operations and maintenance of the MOBLAS-5 system. The MOBLAS-5 crew continues to be one of the top data producing station in the ILRS. The station is continuing three shift operations, seven days per week, twenty-four hours per day.

MOBLAS-6 (Hartebeesthoek, South Africa)

NASA continued its collaboration with the South African National Research Foundation and the Hartebeesthoek Radio Astronomical Observatory (HRAO) for operations and maintenance of the MOBLAS-6 system. The system was originally installed in HRAO in June 2000. The MOBLAS-6 operations began in August 2000. The site dedication ceremony occurred in November 2000. The HRAO site is collocated with Very Long Baseline Interferometry (VLBI), Global Positioning System (GPS), and DORIS. The station is continuing three shift operations, five days per week, twenty-four hours per day.

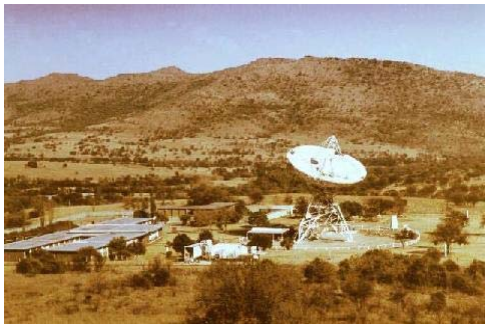

MOBLAS-7 (Greenbelt, Maryland)

NASA continued its collaboration with HTSI for the operations and maintenance of the MOBLAS-7 system. MOBLAS-7 continues to perform outstandingly despite the reduction in operational shifts. The system is used by NASA to test all upgrades and modifications to the NASA network prior to being installed in the field sites. The station is continuing one shift operations, five days per week.

MOBLAS-8 (Tahiti, French Polynesia)

NASA continued its collaboration with Centre National d'Etudes Spatiales (CNES) and the University of French Polynesia (UFP) for the operations and maintenance of the MOBLAS-8 system in Tahiti, French Polynesia. The Tahiti Geodetic Observatory recently named Dr. Jean Pierre Barriot as its new Director. The station was affected by the removal of a NASA operator and trainer due to budget reduction in 2004. The staff has done an excellent job operating and maintaining the station despite poor weather conditions at times. The MOBLAS-8 system was originally shipped to Tahiti in August 1997. The site dedication ceremony occurred in May 1998. The system is collocated with a GPS and DORIS system. The station will be providing two shift operations, five days per week.

TLRS-3 (Arequipa, Peru)

NASA re-newed its collaboration with the Universidad Nacional de San Agustin (UNSA) for the operations and maintenance of the TLRS-3 system in October 2005. The TLRS-3 crew working with Honeywell Technical Solutions Incorporated (HTSI) engineers began restoring the site to full operations. The restoration of the site included repairs to the laser, controller computer, HP5370, gimbal, dome controller, and telescope. The system's first light was September 23, 2006. As of the October 16, 2006, 90 pass segments had been acquired with a data quality of < 10 mm RMS on Lageos. The average ground calibration was at the 5.4 mm level. The station is providing two shift operations, day and night, five days per week.

TLRS-4 (Maui, Hawaii)

NASA renewed its collaboration with the University of Hawaii, Institute for Astronomy (IfA). After the HOLLAS system was decommissioned in June 2004, the site was converted to the new PanStarrs Observatory. NASA decided to bring the TLRS-4 system to operational status and ship it to the Haleakala Observatory in Maui, Hawaii. The TLRS-4 system had a highly successful inter-comparison test with MOBLAS-7. The system passed an Operational Readiness Review in September 2005. After 10 years on non-operations, TLRS-4 was shipped to Maui in April 2006. HTSI working with the University of Hawaii IfA personnel, prepared the site and installed the system on new pad on top of Mount Haleakala. The system's first light was in October 2006. The station will be providing two shift operations, day and night, seven days per week.

MLRS (Fort Davis, Texas)

NASA continued its collaboration with the University of Texas and the Center for Space Research (CSR) for operations and maintenance of the MLRS system in Fort Davis, Texas. MLRS provided SLR and LLR tracking data. CSR continued its data analysis support for the ILRS network. The station will be providing operations seven days per week, twelve hours per day.

Conclusion

The future of the NASA SLR Program is exciting. The resurgence of energy can be seen by the recent accomplishments of the various stations. NASA is increasing its infrastructure as well as plans are in place to increase stations operational shifts. The TLRS-3 system in Arequipa and the TLRS-4 system in Maui will be fully operational in December 2006. Dedication ceremonies for re-opening both sites are being organized for January/February 2007 timeframe. In addition, significant progress continues on the SLR2000 prototype development. We would like acknowledge the extraordinary efforts and dedication of the team supporting the NASA SLR network which includes NASA personnel, contractors, universities, and our foreign partners.

Possibility of Laser Ranging Support For The Next-Generation Space VLBI Mission, Astro-G

Toshimichi Otsubo[1], Toshihiro Kubo-oka[1], Hirobumi Saito[2], Hisashi Hirabayashi[2], Takaji Kato[2], Makoto Yoshikawa[2], Yasuhiro Murata[2], Yoshiharu Asaki[2], and Shinichi Nakamura[3]

1. Kashima Space Research Center, National Institute of Information and Communications Technology, 893-1 Hirai, Kashima 314-8501 Japan
2. Institute of Space and Astronautical Science, Japan Aerospace Exploration Agency, 3-1-1 Yoshinodai, Sagamihara, 229-8510 Japan
3. Consolidated Space Tracking and Data Acquisition Department, Japan Aerospace Exploration Agency, 2-1-1 Sengen, Tsukuba, 305-8505 Japan

Contact: otsubo@nict.go.jp / Fax: +81-299-84-7160

Introduction

Space VLBI (Very Long Baseline Interferometry) missions enable us to extend the baseline length beyond the diameter of the Earth and, as a result, to obtain more precise images of astronomical radio sources. Following the first successful space VLBI mission, HALCA (Hirabayashi, et al., 1998), which launched in 1997 and finished in 2005, JAXA (Japan Aerospace Exploration Agency) approved the next-generation space VLBI satellite called ASTRO-G (Hirabayashi, 2005) in 2006. It is scheduled to be launched in 2012. This new satellite, with a 9.6-metre mesh antenna, will receive high frequency radio signals up to 43 GHz and enhance the resolution of images by approximately 10 times than the former mission. It is expected to provide high-resolution imaging of active galactic nuclei, motion in galactic star forming regions, observations of extragalactic water masers, and so on.

The space VLBI satellite observes stellar objects in collaboration with ground VLBI network. One of the observation modes is called phase compensation observation. That is, the VLBI antenna switches the pointing direction by 2 or 3 degrees every minute to see a target object and a reference object. This makes it possible to compensate the atmospheric delay for ground VLBI stations. In this observation mode, very precise orbits up to a few cm precision are required throughout the trajectory.

Its orbit is highly elliptic. With an eccentricity of 0.62, its altitude varies from 1000 km (perigee) to 25000 km (apogee). The orbital period is about 7.5 hours and the inclination is set to 31 degrees. In contrast to spherical geodetic satellites, the area-mass ratio is large and its shape is very complicated. Therefore, it will experience large and complicated perturbation forces mainly due to solar radiation pressure. Although the cm-order orbit determination for near-circular orbits is nowadays fairly common, that for such an elliptic orbit is a highly challenging problem. We

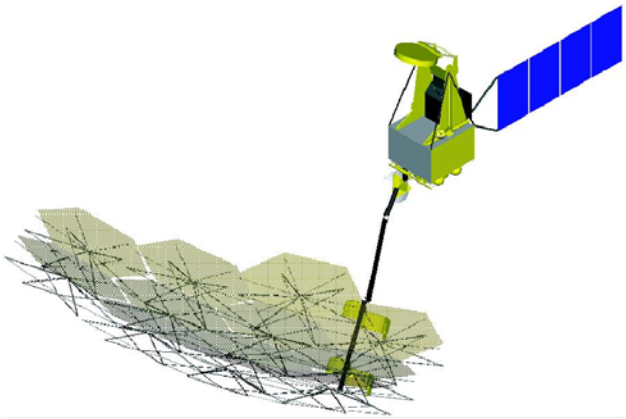

Figure 1. *ASTRO-G satellite.*

are currently investigating possible instruments for high-precision orbit determination. This paper deals a quick-look, first-step simulation of GPS and SLR data.

Possible instruments for precise orbit determination

In the following discussions, we assume these virtual orbital elements of ASTRO-G:

Epoch: 0h UT, 26 Apr 2004
Semimajor axis: 19378 km
Eccentricity: 0.6193
Inclination: 31 deg
Longitude of ascending node: 0 deg
Argument of perigee: 0 deg
True anomaly: 0 deg

After several experiments since 1990's, an onboard GPS receiver is found to be useful for precise orbit determination of low earth orbit (LEO) satellites, and the number of LEO satellites carrying this instrument is rapidly increasing.

We currently consider GPS receiver(s) as the primary instrument for precise orbit measurement. The apogee of ASTRO-G is 25000 km of altitude which is higher than the GPS satellites (20000 km). The beam divergence of GPS microwave signal is almost the size of the earth, so it gets out of the main lobe of the GPS signal (~ 20 degrees for L1 frequency) as its altitude gets high (~ typically a few thousand km).

The number of 'visible' GPS satellites on track was plotted in Fig. 2 using the true GPS constellation on the day. The bottom graph is the geocentric distance of the ASTRO-G satellite. This graph covers 15 hours, almost 2 revolution periods. The 'visibility' is defined so that the ASTRO-G satellite is within the 20-degree beam divergence and it is out of the Earth's shadow. First, assuming a single GPS receiver that always points away from the geocentre, the 'visible' number of GPS satellites is the dotted (blue) line in the top graph. Only when it is close to the perigee, one hour per the 7.5 hours period, it can see more than four satellites. Then, we simulated multiple receivers which provide no limit in terms of direction. The result is plotted as the solid (red) line in the top graph. With the contribution from GPS satellites that locate opposite side of the earth, the 'visible' number increases. Even away from the perigee, a few GPS satellites can be visible, but the number is far less than four in most cases.

In order to overcome this situation, we need to look into the possibility of the use of sidelobe GPS signal. Also, other GNSS satellites like GLONASS and GALILEO are also possible to improve the situation. Nevertheless, we stick to the above condition (solid red line) for the rest of this paper.

In these circumstances, laser ranging seems to play an important role for precise orbits. We have not looked into the specifications, but the reflector array size should be similar to that of GPS or GLONASS satellites. Other possibilities, such as an accelerometer or VLBI delay measurements, are also being considered, but not included in this paper.

Quick-look POD simulations

We simulated the following data set for the 15 hours in Fig. 2:

- GPS: every 30 seconds, pseudorange and carrier phase, L1 and L2 frequency
  (assumed observation error = 10 cm for carrier phase, and 3 m for pseudorange)
- SLR: normal points every 120 seconds
  (assumed observation error = 6 cm)

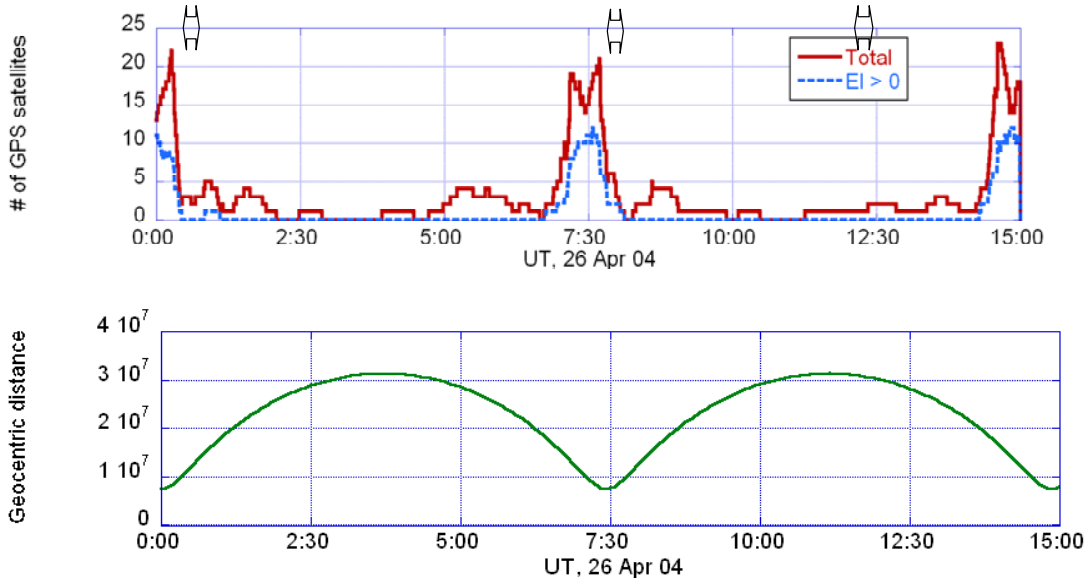

Figure 2. *Number of visible GPS satellites (top) and geocentric distance (bottom) of ASTRO-G simulated orbit. The three two-headed arrows are the duration of assumed SLR observations.*

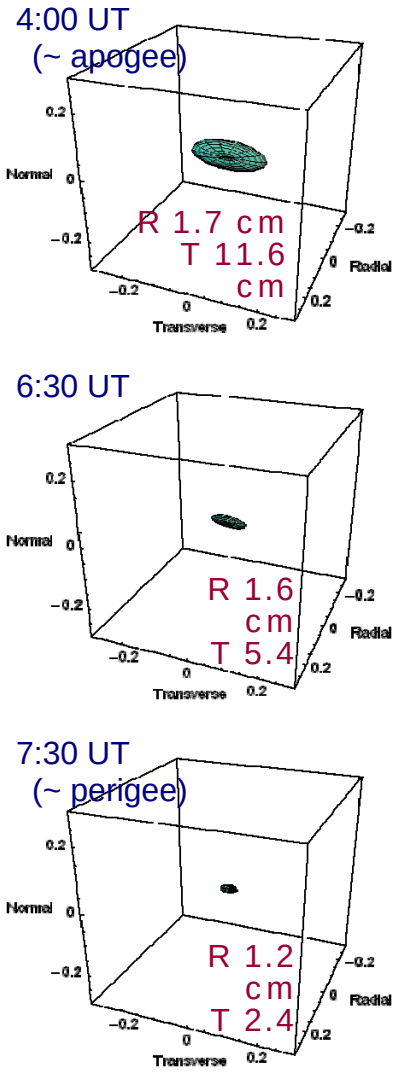

Figure 3. *Error ellipsoids for the GPS-only case.*

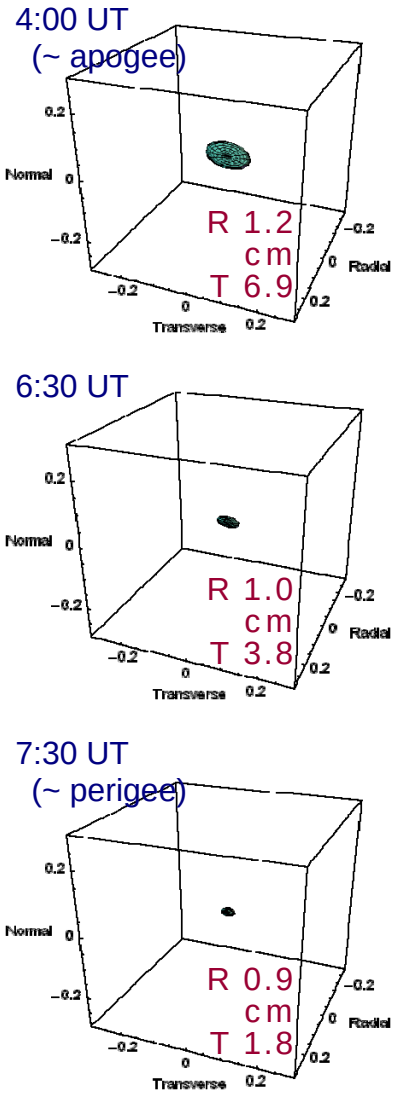

Figure 4. *Error ellipsoids for the GPS+SLR case.*

The orbital parameters, six elements, constant along-track acceleration and once-per-rev along-track acceleration, are estimated at 4:00 (close to the apogee), 6:30 and 7:30 (close to the perigee), instead of the starting time (0:00) of the arc. The clock offsets at each epoch and the ambiguities of ion-free GPS carrier phase are also solved for. We look into the covariance matrix of the orbit positional solution to obtain the estimation error. The covariance matrices given in the XYZ inertial coordinate system are then converted to the RTN satellite-fixed system, that is, in Radial, Transverse and Normal direction.

We firstly simulated the GPS data only. The ellipsoidal bodies in Fig. 3 show the size of three-dimensional errors for the three epochs. The error in the transverse component (= along-track component at the apogee and the perigee) is dominant in all cases. As expected, the ellipsoid gets larger around the apogee where GPS signal is merely detected.

Then we added the SLR data, the three 30-minute passes shown in Fig. 2, to the GPS data. The ellipsoids are shown in Fig. 4. It is obviously seen that the errors in the transverse and radial components are significantly reduced by the addition of the small amount of SLR data. Although we cannot expect dense tracking from the SLR network, this result suggests the SLR data will significantly contribute to the improvement of the orbit of ASTRO-G.

Discussions for future studies

The precise orbit monitoring instrument for the ASTRO-G satellite is being investigated. SLR observations will significantly improve the orbit compared to the GPS-only case. With further analyses we need to consider the details on the instruments such as the number and arrangement of GPS antennas and SLR retroreflectors.

The International Laser Ranging Service (ILRS) had a small experience of highly elliptic orbit satellite in the LRE (Laser Ranging Equipment) test mission launched to a geostationary transfer orbit in 2001 (Otsubo, et al., 2002). If the satellite actually carries retroreflectors for SLR, we would like to ask the ILRS stations to adapt their tracking system to highly elliptic orbits.

Due to the complicated shape of the satellite and the large area-per-mass ratio, this satellite is to experience largely complicated perturbation forces from solar radiation pressure that is about 100 times of LAGEOS. Therefore, along with the orbit measurement instruments discussed in this paper, the establishment of a precise force model is also essential for the precise orbit determination of this satellite.

References

[1] Hirabayashi, H., H. Hirosawa, H. Kobayashi, Y. Murata, P. G. Edwards, E. B. Fomalont, K. Fujisawa, T. Ichikawa, T. Kii, T. Lovell, G. A. Moellenbrock, R. Okayasu, M. Inoue, N. Kawaguchi, S. Kameno, K. M. Shibata, Y. Asaki, T. Bushimata, S. Enome, S. Horiuchi, T. Miyaji, T. Umemoto, V. Migenes, K. Wajima, J. Nakajima, M. Morimoto, J. Ellis, D. L. Meier, D. W. Murphy, R. A. Preston, J. G. Smith, S. J. Tingay, D. L. Traub, R. D. Wietfeldt, J. M. Benson, M. J. Claussen, C. Flatters, J. D. Romney, J. S. Ulvestad, L. R. D'Addario, G. I. Langston, A. H. Minter, B. R. Carlson, P. E. Dewdney, D. L. Jauncey, J. E. Reynolds, A. R. Taylor, P. M. McCulloch, W. H. Cannon, L. I. Gurvits, A. J. Mioduszewski, R. T. Schilizzi, R. S. Booth, "Overview and Initial Results of the Very Long Baseline Interferometry Space Observatory Programme," Science, 281, 1825, 1998.

[2] Hirabayashi, H., "Next Generation Space VLBI," EAS Publications Series, 15, 465-478, 2005.

[3] T. Otsubo, H. Kunimori, K. Yoshihara, H. Hashimoto, "Laser Reflector Arrangement on H2A-LRE Satellite for Monitoring the Spin Rate and the Optical Degradation," Applied Optics, 41, 27, 5672-5677, 2002.

Electron Multiplying CCD Camera Performance Tests

D. Lewová[1], M. Němec[1], I. Procházka[1], K. Hamal[1],G. Kirchner[2], F. Koidl[2], D. Kucharski[3], Yang Fumin[4]

1. Czech Technical University in Prague, Brehova 7, 115 19 Prague 1, Czech Republic,

2. Graz Observatory, Austrian Academy of Sciences, Austria

3. Space Research Centre, Polish Academy of Sciences, Poland

4. Shanghai Observatory, Chinese Academy of Science, China

Contact: lew.dana@gmail.com , nemecm1@troja.fjfi.cvut.cz

Abstract

For satellite laser ranging, TV guiding is widely used to point the laser beam on the satellite. The ISIT (Intensified Silicon-Intensifier Target) camera has been applied in last years for its high sensitivity, which enabled to track all satellites of interest. However, there is a strict limitation to use it for daylight observation. The new type of CCD camera Electron Multiplying CCD (EMCCD) provides high sensitivity for short integration time required for fast real time tracking while maintaining the high ruggedness for daylight tracking. An additional internal gain reaches a factor up to 200 in comparison with regular CCD. During our tests in Graz and Shanghai, we did demonstrate the ability for satellite laser ranging during the daylight and during the night time exploiting the higher sensitivity, as well. The test results and a comparison with ISIT technology will be presented.

EMCCD Camera Performance Tests

- EMCCD provides high sensitivity for short integration time required for fast real time tracking
- In comparison with ISIT, EMCCD offers adjustability of exposure time and EM gain and beside the Analog video output it has very fast native Digital output allowing better image enhancement post-processing
- During our tests in Graz and Shanghai we did demonstrate the ability for SLR during daylight and night operations

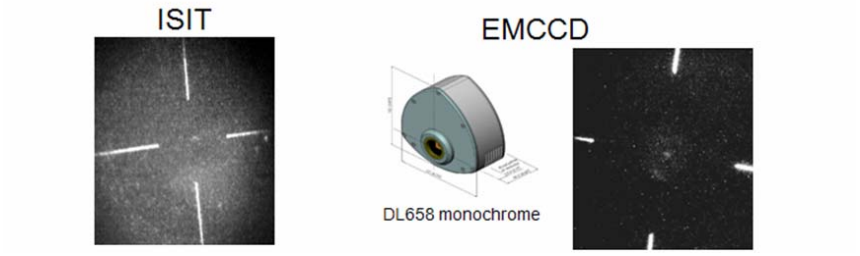

EMCCD Camera Performance Tests

EMCCD Images of GPS, Etalon 2, Glonass and Lageos 2 illuminated by Sun only

Digital output – no enhancement
(Images are captured with the same EMCCD settings and inverted)

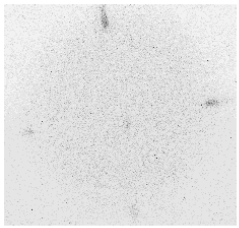

Gps BIIA-24, 0.2s, Gain 250
2006-08-25T20:07:39 UTC
Sun only, Altitude ~ 20,100 km

10x10pixels	Object	Backgr.
Standard Deviation	350,37	243,86
Mean	939,13	818,49
Maximum	2603	2263
Total Counts	375652	327396

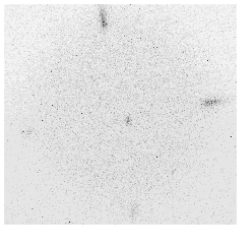

Etalon2, 0.2s, Gain 250
2006-08-25T20:39:42 UTC
Sun only, Altitude ~ 19,100 km

10x10pixels	Object	Backgr.
Standard Deviation	471,25	274,1
Mean	1024,35	820,27
Maximum	4129	2119
Total Counts	375652	328106

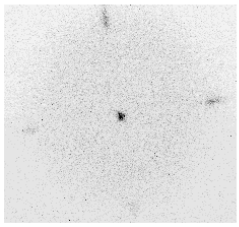

G87- Glonass, 0.2s, Gain 250
2006-08-25T22:53:02 UTC
Sun only, Altitude ~ 19,100 km

10x10pixels	Object	Backgr.
Standard Deviation	1508,39	310,89
Mean	1870,07	869,8
Maximum	10835	2235
Total Counts	748028	347920

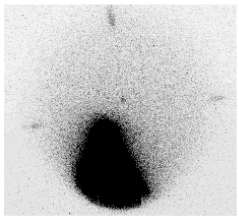

Lageos2, 0.2s, Gain 250
2006-08-25T19:27:57 UTC
Sun only (Laser outside the object)
Altitude ~ 5625 km

10x10pixels	Object	Backgr.
St. Deviation	629,62	503,65
Mean	1713,28	1495,48
Maximum	4375	3389
Total Counts	685310	598194

EMCCD Camera Performance Tests

Analog video output enhancement

On-line video filter - Contrast enhancement
GPS 36

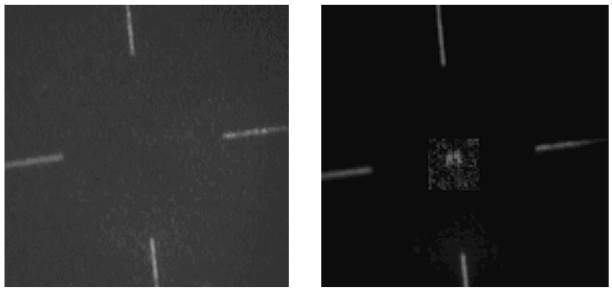

before | after

On-line video filter - Pseudocolor mapping

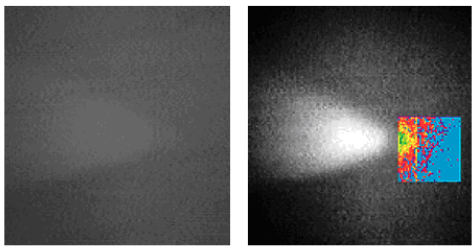

before | after

For more details see the following Poster.

Electron Multiplying CCD Camera Performance Tests

D. Lewova, M. Němec, I. Procházka, K. Hamal (1)
G. Kirchner, F.Koidl (2)
Yang Fumin(3), D. Kucharski (4)

(1) Czech Technical University in Prague, Czech Republic, (2) Satellite Laser Station Graz, Austrian Academy of Sciences, Austria
(3) Chinese Academy of Sciences, Shanghai, China, (4) Space Research Centre, Polish Academy of Sciences,Poland

For satellite laser ranging, TV guiding is widely used to point the laser beam on the satellite. The ISIT (Intensified Silicon-Intensifier Target) camera has been applied in last years for its high sensitivity, which enabled to track all satellites of interest. However, there is a strict limitation to use it for daylight observation. The new type of CCD camera Electron Multiplying CCD (EMCCD) provides high sensitivity for short integration time required for fast real time tracking while maintaining the high ruggedness for daylight tracking. An additional internal gain reaches a factor up to 200 in comparison with regular CCD. During our tests in Graz and Shanghai we did demonstrate the ability for satellite laser ranging during the daylight and during the night time while exploiting the higher sensitivity , as well. The test results and a comparison with ISIT technology will be presented.

Andor Luca DL658 (monochrome)

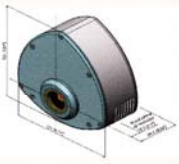

Technology	Electron Multiplying CCD ("gain off" operable)
Active Pixels (horiz x vert)	658 x 496
Pixel Size (horiz x vert; µm)	10 x 10
Image Area (mm)	6.58 x 4.96
Sensor	TIL
Peak Q.E.	52%
Minimum Oper. Temp (°C)	-20
Active Area Pixel Well Depth(e⁻ typical)	25,000
Conventional Register Pixel Well Depth (e⁻ typical)	100,000
Pixel Readout Rate	12.5
Read Noise (e-)	25
Min Operating Temp (°C)	-20
Digitization	14-bit
Max. Frame rate	30 full frames/sec
PC Interface	USB 2.0 only
Price	$8850 / €7500
Software	Solis (Not Recommended) $1500 / €1400

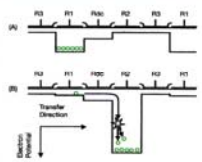

Gain register operation

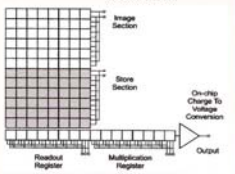

EMCCD structure

EMCCD Camera Tests

Shanghai Observatory

Graz Observatory

Test conditions:

optics	Canon lens TV-16, 1;1.4, f=50 mm, C-mount
optics settings	f/D = 22, additional ND filters 12 x each, 3 pieces
signal source	red LED, 7m distance, dark room
software	ANDOR Solis for imaging, ver. 4.3.0.0
PC notebook	UMAX Vision Book 632LX, Celeron D, 2.5GHz, 512 MB,USB2.0

EMCCD and ISIT, Graz, 2006

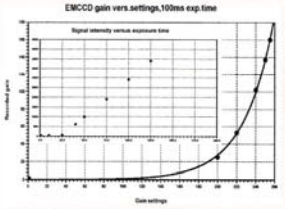

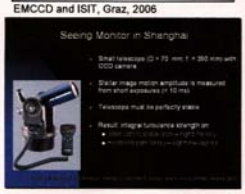

ISIT vs. EMCCD Comparison

GPS-36 25.8.2006 22:08 Local time

Satellite object max/background level : 1,3

ISIT
only night observation
high FPS (30)

Satellite object max/background level : 3

EMCCD
Negs.:
night + day observing
up to 30 FPS
only 5 FPS
(for the same results)
EM ageing / anti-ageing
Pros.:
lower sensitivity
lower noise (EM gain on)
adjustability of exposure time and EM gain

EMCCD Gain experiment :

- green LED
- additional 2 ND filters inserted into optical path
- exposure time set to 100 ms
- the "EMDAC setting" set to values in the range of 1 to 255

Exposure time linearity:

- the gain setting =1 (no EM additional gain)
- one ND filter inserted into optical path
- the image intensity evaluated as a function of image exposure time (linear dependence expected)
- the gain increases with exposure time starting at 1 ms exposures
- the gain increase is linear only for exposure times >= 25 ms !

Gps BIIA-24, 0.2s, Gain 250
2006-08-25T20:07:39 UTC
Sun only, Altitude ~ 20,100 km

10x10pixels	Object	Backgr.
Standard Deviation	350,37	243,86
Mean	939,13	818,49
Maximum	2603	2263
Total Counts	375652	327396

Etalon2 0.2s, Gain 250
2006-08-25T20:39:42 UTC
Sun only, Altitude ~ 19,100 km

10x10pixels	Object	Backgr.
Standard Deviation	471,25	274,1
Mean	1024,35	820,27
Maximum	4129	2119
Total Counts	409740	328106

G87- Glonass, 0.2s, Gain 250
2006-08-25T22:53:02 UTC
Sun only, Altitude ~ 19,100 km

10x10pixels	Object	Backgr.
Standard Deviation	1508,39	310,89
Mean	1870,07	869,8
Maximum	10835	2235
Total Counts	748028	347920

Lageos2, 0.2s, Gain 250
2006-08-25T19:27:57 UTC
Sun only (Laser outside),
Altitude ~ 5625 km

10x10pixels	Object	Backgr.
St. Deviation	629,62	503,65
Mean	1713,28	1495,48
Maximum	4375	3389
Total Counts	685310	598194

Data Mining - HW

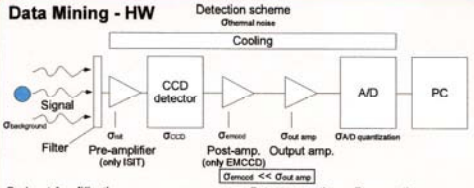

Pre/post Amplification
- decreasing readout noises levels (Low-noise internal amplification of signal before high-noise external output amplification)
- Increasing influence of S/N

Detectors settings - Exposure time
- Internal binning
- Post/pre amplifications

Filtration - interested wave-lengths pass only
- background influence(level) elimination

Cooling - Decreasing thermal noises

GPS BIIA-24 on-line filter
2006-08-25T22:09:39 UTC
Averaging - 25 frames
Selected area – contrast enhanced

Adjusted Contrast and brightness in the selected area

PC – Software methods

Methods for S/N increasing :
SW binning – 3D (integration in time + 2D in space)
SW Exposure - summation of frames
Averaging (mean; time)
Flatfield – Intensity levels calibration
Background Reduction
- Bcg. Frame subtraction(frame without object)
- AVG Filter } Artificial Background estimation and subtraction
- Median Filter

Visualization

Methods for better visibility of objects in real time :

Levels selection - Image histogram
Adjusting of contrast and brightness
Gama correction
Color inverting
Pseudo-color mapping

Pseudo color mapping

40W, 2J laser Moon shooting

Shanghai observatory

Replacing dichroic mirror

During tests in Graz and Shanghai we did demonstrate the ability for satellite laser ranging during the daylight and during the night time while exploiting the higher sensitivity

LIDAR Experiments At The Space Geodesy Facility, Herstmonceux, Uk

Graham Appleby[1], Christopher Potter[1], Philip Gibbs[1] and Roderic Jones[2]

1. NERC Space Geodesy Facility, Herstmonceux, Hailsham, UK

2. Department of Chemistry, University of Cambridge, Lensfield Road, Cambridge, UK

Introduction

We are developing a LIDAR capability, ultimately to run concurrently with satellite laser ranging measurements, at Herstmonceux, UK. Our interest is in monitoring atmospheric pollution, boundary layer heights and cirrus properties over the site. For preliminary testing we have developed a modified version of the laser ranging software and used the existing laser ranging hardware to detect backscatter at a range of heights of from one to 14 km vertically above the site. During experimental runs the C-SPAD detector is gated in few-hundred metre increments from close to the telescope to beyond the tropopause, and time-tagged single-photon backscatter events are detected. Over the experimental period of a few minutes a vertical profile of atmospheric response is mapped and various layers detected. In this paper we discuss some analysis of these preliminary results and state plans for future enhancements.

Backscatter experiments

With the telescope set towards the zenith, we gate the C-SPAD for usually 30-seconds at each height above the site, from 1000 to 14,000m and collect backscatter events. The initial height of 1000m is imposed on this experiment by the separation between the transmit-receive telescopes, whose fields-of-view begin to intersect about 800m from the mount.

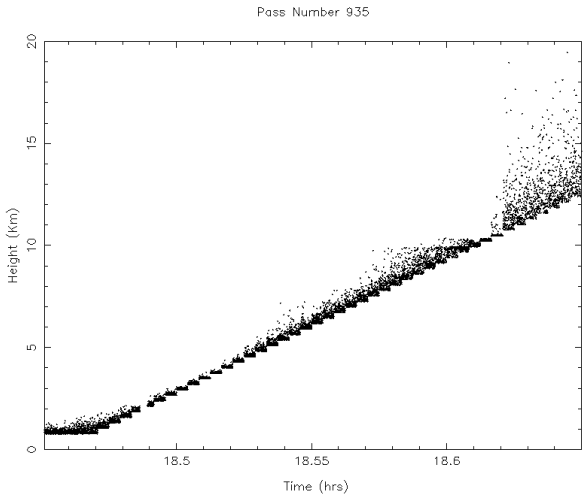

Figure 1. *Raw observations of backscatter events vertically above Herstmonceux*

The plot in Figure 1 shows the 'stepladder' that results when the raw event-height results are plotted against time. During the setup process at the first height, neutral density filters (ND) were entered manually into the receiver optical path to ensure that the range gate was approximately uniformly filled with events. Thereafter, ND values were not changed.

Preliminary analysis

We carry out a preliminary analysis of the backscatter measurements by taking the raw observations and computing for each noise point its distance above the station, on the assumption that for night-time observations all data shown in Figure 1 result from laser backscatter in the atmosphere. On this assumption and, at this stage, ignoring the decrease of laser energy with height, we therefore are able to measure return energy as a function of height and thus probe atmospheric particulate density.

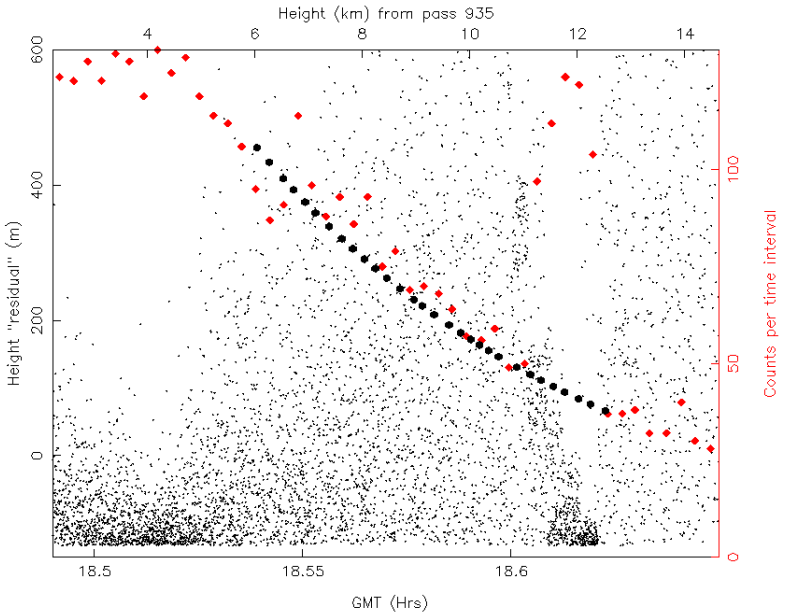

Figure 2. *Backscatter events plotted as a function of time and height in the atmosphere*

Figure 2 shows the results of this simple analysis applied to the observational session of Figure 1. If the degree of backscatter from the atmosphere was independent of height, the plot would show a uniform density of points. However, this is clearly not the case, and from the plot we suggest that a haze layer can be seen at about 4-5Km above the site, followed by a further layer at 12 km, probably identified with the tropopause. The red dots, plotted against the right-hand vertical axis, give the total number of events detected in each 3-minute interval throughout the experiment. We have fitted to those red points, strictly between the two haze layers (6 to 11km), the exponential decay curve shown by the black dots, and determine from it an atmospheric scale height of approximately 6km. Note that this fitted curve is extended in the plot beyond the region of the fit, through the high level layer, where it links with the observational totals for 13km and above. More work will be required to refine this analysis, in particular to estimate the decrease of laser energy with height.

Monitoring cloud and contrail optical density

In a related study, we are interested in the possibility of monitoring contrail and cirrus optical depth during standard laser ranging. The airspace over Herstmonceux is a busy flight path to Gatwick as well as a gateway into the UK for transatlantic routes, and a recent study into contrails over this part of the country (Stuber *et al*, *NATURE*, June 2006) has highlighted the importance of contrails as contributions to warming effects. However, little is known about the characteristics of contrails, and estimates of their optical depth vary greatly.

During laser ranging, the tracking software automatically maintains the average return level at single photons by inserting varying degrees of ND filters in the detector optical path. Compared with a model of the link budget for the ranging process, the degree of ND actually required to achieve single photon returns is a measure of departure of atmospheric transparency from that in the model. In particular, if the pass transits a contrail, the required change (reduction) in ND necessary to maintain single photon returns is a direct measurement of the additional optical depth of the atmosphere due to the trail.

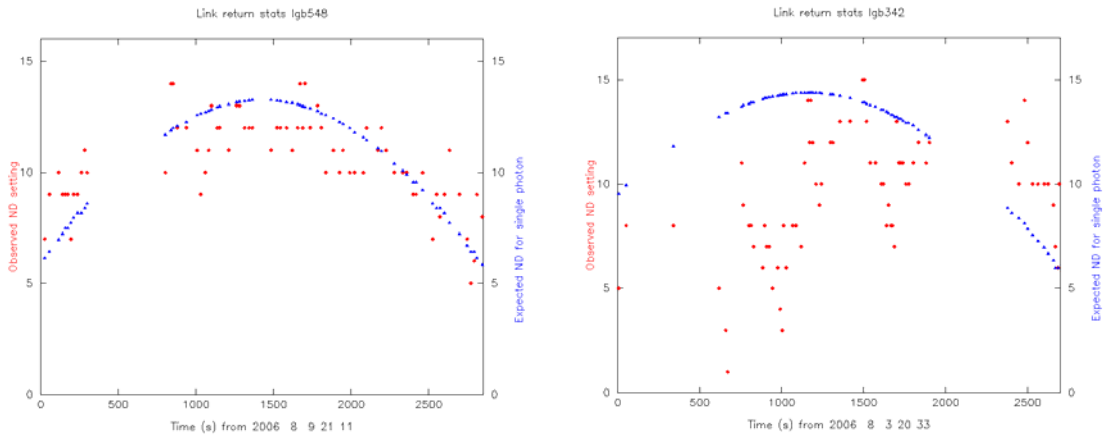

***Figure 3**. Comparison of theoretical (blue) and measured (red) ND required for single-photon laser return from LAGEOS-2.*

The plots in Figure 3 above show two tracking instances of modelled (blue points in smooth curves) and actual ND (red, scattered points) inserted by the operating system; the left plot is in a clear sky and the right plot shows three passages of the satellite behind contrails. The clear sky data follows the predicted ND values fairly well, the small changes being due to pointing variations from optimal. During the contrail passages, ND is systematically removed and replaced, giving a profile of contrail optical density.

Conclusion.

Both the observational experiments reported in this paper are at preliminary stages. Much more work is required to improve and automate the observational methods, quantify systematic effects and analyse the results. We also plan to design and integrate on the telescope a LIDAR system that is independent of, but which will run simultaneously with, standard laser ranging operations.

Possibility of the Near Earth Objects Distance Measurement with Laser Ranging Device

M.Ābele, L.Osipova

Institute of Astronomy, University of Latvia, Raiņa bulv. 19, Rīga LV-1586, Latvia

Abstract

The orbit perihelion of a some of minor planets is nearer from the Sun than the Earth's orbit. Observations are possible only in a small part of the orbit. Orbital elements of them cannot be determined accurately because we have only angular coordinates. The use of a laser ranging device for distance measurements will greatly improve the precision of determining orbital elements.

Keywords: *minor planets, laser ranging*

Introduction

We know a number of minor planets whose orbital perihelion is nearer from the Sun than the Earth's orbit.[1] Accurate forecasting of their motion is not possible, because they can be observed only in the vicinity of aphelion when their lighted sides are turned toward the Earth, and the Sun is located on the opposite side. Observations are possible only for a small part of the orbit because the planets are small in size and it is not possible to observe them from the Earth even with powerful telescopes. In order to determine orbits more accurately, we assess the possibility to measure the distance to these orbits with a laser ranging device. [2, 3, 4]

Possible measurements of minor planets with laser ranging device

A possible scheme of the experiment is shown in Fig. 1. The laser device LAS, which is situated on the Earth, radiates impulses of light in the direction of the minor planet MP. The distance is L and the diameter of the laser beam is d_{la}:

$$d_{la} = 2 \cdot L \cdot \mathrm{tg}\, r_d \tag{1}$$

where r_d is the diffraction, the angle radius $r_d = 1.2197\ \lambda/d_t$ that depends on the radiation optics' diameter d_t and the wavelength λ [5].

As the energy l_i diffraction image is irregular, the energy radiated in the direction of the minor planet E_{ep} can be calculated using formula

$$E_{ep} = E_{las} \cdot c_{at} \cdot c_{op} \frac{\int_0^{d/2} l_i(r) \cdot r \cdot dr}{\int_0^{r_d} l_i(r) \cdot r \cdot dr} \tag{2}$$

where E_{las} – laser emanated energy;

c_{at} – light transmissivity of the atmosphere;

c_{op} – light transmissivity of the optical system;

d – diameter of the minor planet.

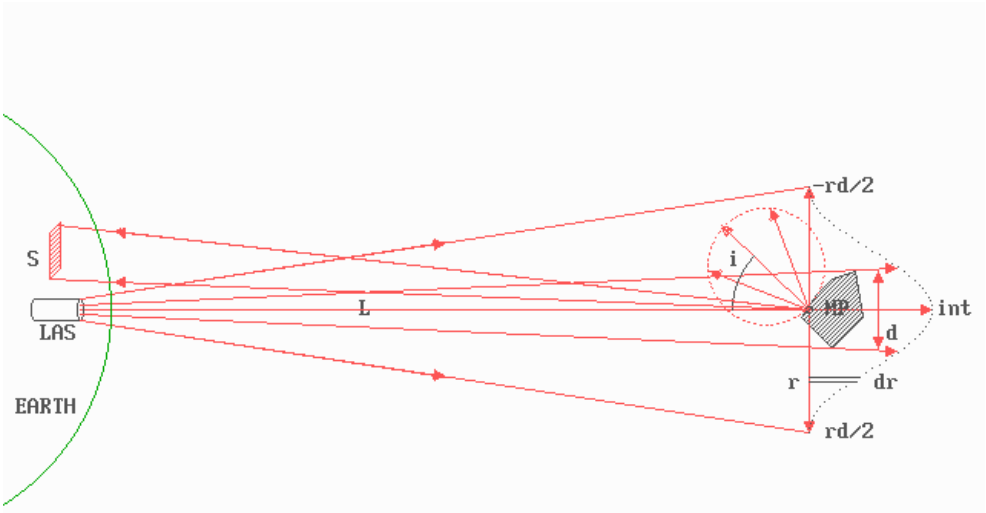

Fig. 1. Measurments of minor planets with laser ranging device

The surface of the minor planet is matted and its each element reflects the light in accordance with the Lambert Law. Area S on the Earth receives radiated energy E_e:

$$E_e = E_p \cdot c_{at} \cdot a \cdot \cos i \cdot \frac{S}{\pi L} \qquad (3)$$

where i – mean surface normal angle turned in the direction of the Earth;

a – reflection coefficient (albedo).

As E_e is very weak, the reflected energy can be described with the number of photons per unit of area $n_f = E_e/E_{fot}$, where E_{fot} – photon energy:

$$E_{fot} = h \cdot \nu \qquad (4)$$

where h – Planck's constant ($h = 6.622 \cdot 10^{-34}$ J·s);

ν – frequency of light wavelength.

The calculation results are showed in Table 1:

Laser energ. = 10 J

Laser wave length = 0.694 mkm

Laser beem diverġence = 0.5819907" (2 r difr)

Atmospher transmitance = 0.8

Telescope transmitance = 0.9

Planets albedo = 10 % (black)

	Planets diameter, m				
	50	100	200	400	800
Range, km	Reflected photons on 1 km^2				
50000	1.953181E+7	6.593346E+7	1.413264E+8	1.583503E+8	1.631335E+8
100000	1275306	4882952	1.648337E+7	3.53316E+7	3.598758E+7
200000	80588	318826	1220738	4120841	8832901
400000	5052	20147	79706	305184	1030210
800000	316	1263	5036	19926	76296
1600000	19	79	315	1259	4981
3200000	1	4	19	78	314
6400000	0	0	1	4	19
1.28E+7	0	0	0	0	1
2.56E+7	0	0	0	0	0

Table 1*. Reflected photons from minor planet.*

The minor planet is irradiated by the Sun. Energy received by the minor planet per second is:

$$E_{sp} = W_s \cdot \pi \cdot \frac{d^2}{4}\ , \tag{5}$$

where W_s – constant of the Sun (near the Earth W_s = 1360 W/m^2).

Of late, CCD devices with very high sensitivity in red waveband 0.694 μm wavelength laser have been used. In this waveband, the Sun's radiation is less intense than in the visible range. If wavelength is dλ, energy in the zone is

$$\varepsilon_\lambda = \frac{2\pi hc^2 \cdot d\lambda}{\lambda^5 \cdot e^{\frac{hc}{\lambda kT}} - 1}\ . \tag{6}$$

Energy of the reflected light is

$$E_{st} = E_{sp} \cdot \frac{\varepsilon_\lambda}{\varepsilon} \cdot c_{at} \cdot a \cdot \cos i \cdot \frac{S_{tr}}{\pi L}\ , \tag{7}$$

where S_{tr} is the area of the reflected light:

$$S_{tr} = \pi \cdot \frac{D_{dt}^2}{4}\ . \tag{8}$$

And the frequency f_n is

$$f_n = \frac{E_{st} \cdot q}{E_{fot}}\ , \tag{9}$$

where q – receiver quantum efficiency.

The probability that at least one photon enters the telescope aperture is small. If a telescope with 1.6 m diameter is used, about 50 reflected pulses may be detected in one hour, the noise from the solar background is 249 pulses per second on the average. If a larger receiving telescope is used, a minor planet's trajectory can be spotted better, the measurements can be done at a larger distance and the reflected pulses received with a higher frequency (Fig. 2).

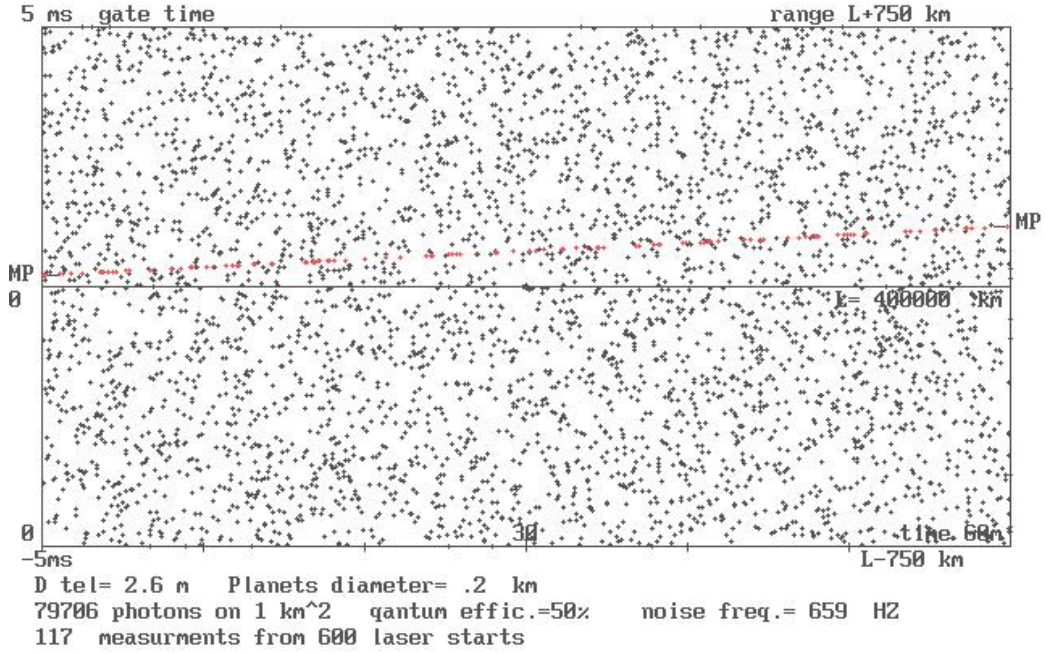

Fig.2. Reflected laser pulses and noise from minor planet

Experiment realization possibility

Described experiment is in planning stage. In order to ensure irradiation of the minor

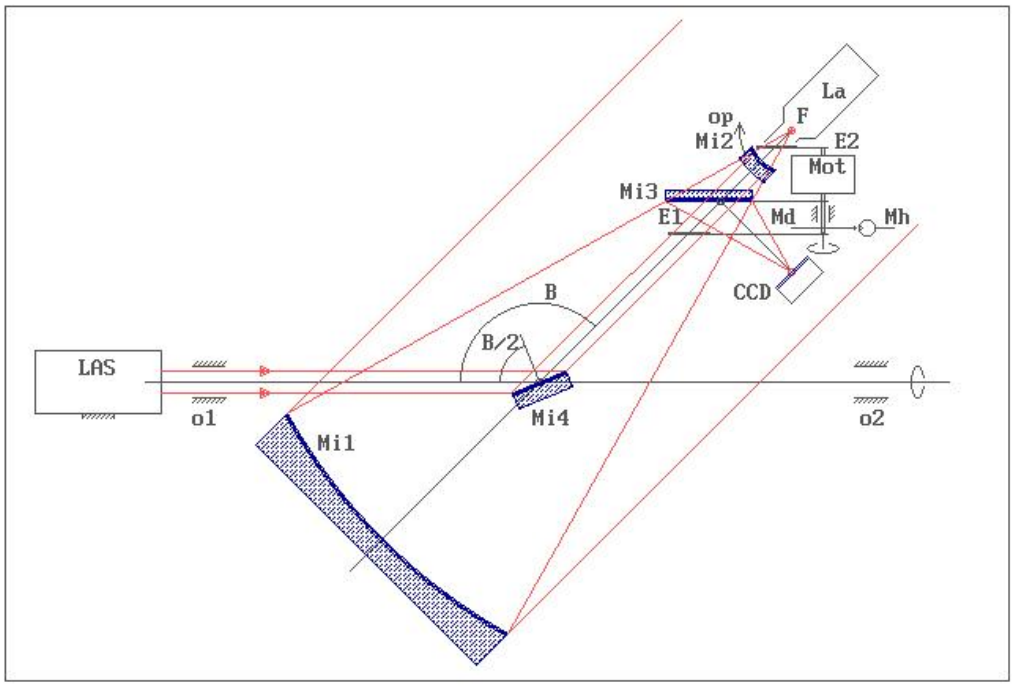

Fig.3. The laser arangement relative to the telescope

planet with a laser beam, a telescope for lighting up cosmic objects from the Earth is being devised at the Institute of Astronomy of the University of Latvia [Fig. 3, 4].

Its main optical element is the paraboloid mirror, 600 mm in diameter, that is put in a special mounting with a horizontal first axis of mounting. It allows for the laser beam to be directed to the irradiation object by a single additional mirror. [6] A laser device with the power level of 10 J can be manufactured in Lithuania by EKSPLA Company.

The receiver telescope of the reflected signal can be placed in a large distance from the transmitting source. Any astrophysical telescope with a mirror of over 1 meter in diameter could be used, and the 1.6 m telescope of the Moletai Observatory (Lithuania) could be a good option. In order to minimize the signals reflected from the Sun, for background impulses the exit of the telescope needs to be equipped with the narrow-band light filter.

Fig.4*. The telescope model.*

Taking into account that the transmitting and receiving devices are situated in a large distance each from the other, it is difficult to harmonize their frequency ranges. The frequencies of transmitted and reflected energy may also differ due to the Doppler Effect. Therefore, it is convenient to make use of a spectrograph with its exit equipped with a charge coupled device (CCD) camera. The scheme of the measurement device is showed in Figure 5.

The spectrum of the minor planet is projected on the outer column of the charge matrix CCD. At the time moment when the re-transmitted impulse from the planet can be expected, a frequency from the silica generator GEN, which moves the accumulated information along j axis, is supplied by the help of an electronic switch whose operation has been synchronized with the GPS time scale. When all matrix cells are filled consistently with the ordinary algorithm with the help of the synchronization scheme SINH through a digital amplitude modifying device, the matrix content is fed to the computer DAT. The available information covers ~ 1000

spectrum zones. One of them can capture the retransmitted impulses from the surface of the minor planet. Any needed zone can afterwards be found from within the absorption zones of the Sun. If a frequency that shifts information from one matrix column to another is 15 MHZ, the distance measurement discreet is 10 m. This allows realization of the showed algorithm of measure.

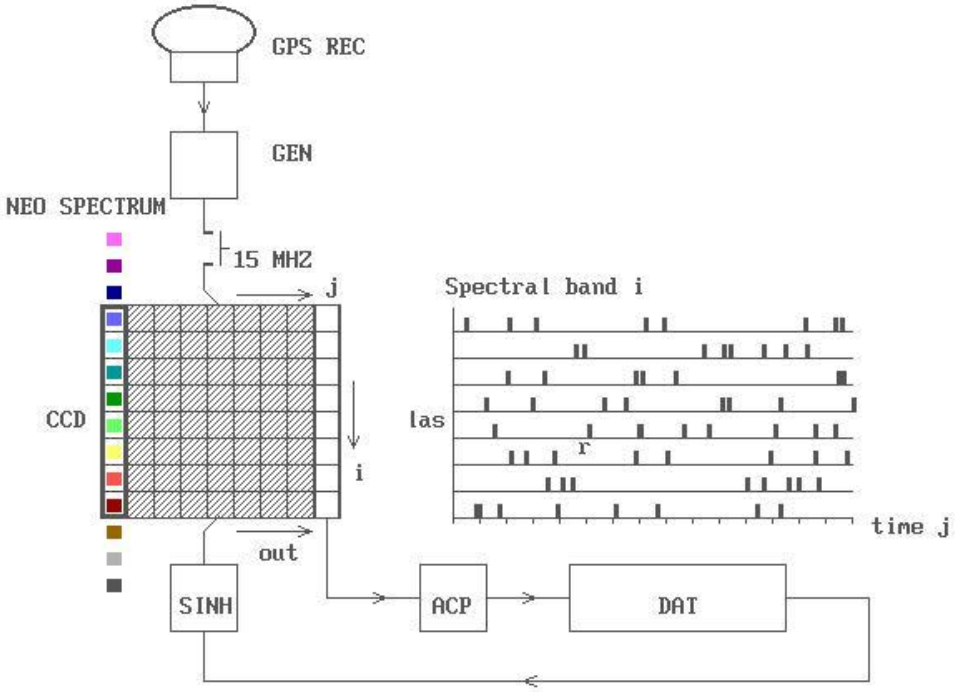

Fig. 5. Spectrograph for reflected pulses measurment

Conclusions

This project can be carried out in co-operation with other astronomers of the Baltic States. Its implementation would enable scientists to improve significantly the orbital elements of the minor planets that present danger to the Earth and to forecast their motion in the future.

References

[1] IAU Minor Planet Center. Unusual Minor Planets. 2002 Sept. 10. http://cfa-www. harvard. edu/iau/lists/Unusual. html

[2] Abele M., Osipova L. Determination of NEO orbits based on laser ranging measurements. Latvian Journal of Physics and Technical Sciences. 2004. 1. p. 31-36.

[3] Abele M., Balklavs-Grinhofs A., Osipova L. Possibility of minor planets distance measurement with laser ranging device. Latvian Journal of Physics and Tehnical Sciences. 2004. 2. p. 54-61,

[4] Degnan John J. Unified Approach to Photon-Couting Microlaser Rangers, Transponders, and Altimeters. Surveys in Geophysics Kluver Academic Publishers. 2002.

[5] Д.Д.Максутов. Астрономическая оптика. 1946. (rus.)

[6] Abele M., Vjaters J., Ubelis A., Osipova L. A telescope to spot space objects from the Earth surface. Latvian Journal of Physics and Tehnical Sciences. 2005. 3. p. 20-28.